

Perturbative EFT calculation of the deuteron longitudinal response function

Andrew J. Andis,^{1,*} Songlin Lyu (吕松林),^{2,3} Bingwei Long (龙炳蔚),^{4,5} and Sebastian König^{6,†}

¹*Department of Physics and Astronomy, North Carolina State University, Raleigh, North Carolina 27695, USA*

²*Dipartimento di Matematica e Fisica, Università degli Studi della Campania “Luigi Vanvitelli”, viale Abramo Lincoln 5 - I-81100 Caserta, Italy*

³*Istituto Nazionale di Fisica Nucleare, Complesso Universitario di Monte S. Angelo, Via Cintia - I-80126 Napoli, Italy*

⁴*College of Physics, Sichuan University, Chengdu, Sichuan 610065, China*

⁵*Southern Center for Nuclear-Science Theory (SCNT), Institute of Modern Physics, Chinese Academy of Sciences, Huizhou 516000, Guangdong, China*

⁶*Department of Physics, North Carolina State University, Raleigh, North Carolina 27695, USA*

In this work, we study the longitudinal response function of the deuteron up to next-to-next-to-leading order in chiral effective field theory (Chiral EFT). We use an approach that maintains exact renormalization group (RG) invariance at each order of the EFT expansion by treating all subleading corrections in perturbation theory. To that end, we extent the Lorentz Integral Transform (LIT) method to allow for such a perturbative treatment. In doing so, we further develop the existing work on strictly RG invariant Chiral EFT, which has so far focused primarily on binding energies and static properties, to inelastic processes. We carefully analyze the convergence properties of the theory and find good agreement with available experimental data. Our findings provide the foundation for similar studies of inelastic processes in a range of nuclei, based on perturbatively renormalized EFT schemes.

I. INTRODUCTION

Nuclear effective field theories (EFTs) are a cornerstone of modern low-energy nuclear theory because they enable calculations of atomic nuclei to be described as fully dynamical few- and many-body systems of protons and neutrons with interactions between the nucleons derived as a systematic approximation of Quantum Chromodynamics (QCD). The approximation takes the form of an expansion in powers of Q/M_{hi} , where Q is the typical size of momenta of the particles involved in the processes of interest and M_{hi} is the breakdown scale of the EFT that is associated with, *e.g.*, the mass of the heavy particles or the energies of some highly excited states that are “integrated out.” Although the physics associated with these scales does not enter explicitly, their effects on low-energy observables are encoded in the coupling strengths of various contact (zero-range) interactions within the EFT.

Of the various EFTs relevant for low-energy nuclear structure and reactions, most recently reviewed in Ref. [1], the so-called Chiral EFT (ChEFT) is generally assumed to be applicable for describing a significant fraction of the chart of nuclides. Based on the assumption that the (approximate) chiral symmetry of QCD, $SU(2)_L \times SU(2)_R$, is spontaneously broken, one can write down a Chiral Lagrangian that manifests this symmetry in terms of the pionic and nucleonic degrees of freedom [2–6]. This approach then describes the strong interactions between nucleons, and also electroweak processes [7–14]. Even extensions beyond the Standard

Model can be included in the Chiral Lagrangian; see, for example, Refs. [15–18]. However, the EFT Lagrangian has in principle an infinite number of operators, and therefore one needs an organization scheme, the so-called power counting, to decide which operators in the Lagrangian are needed for a desired target precision of observables calculated from the EFT.

In the most simple scheme, referred to as naive dimensional analysis (NDA), one counts the dimension of operators in the Lagrangian, built from a combination of fields, and derivatives acting on them (or momenta multiplying them, if the theory is formulated in momentum space), and then one places powers of M_{hi} in the denominators to fix the overall dimension of the term with a dimensionless coupling strength. Although popular in applications of ChEFT to nuclear physics, NDA can be unreliable because other soft mass scales, such as the pion decay constant f_π , are present in the theory and therefore an operator may be related to Q/f_π rather than the suppressed ratio Q/M_{hi} . It is possible to use Renormalization Group (RG) invariance to identify enhancement of interactions terms relative to NDA *before* one even confronts the EFT with experimental data. For example, the RG constraint—*i.e.*, that observables are insensitive to an arbitrarily chosen ultra-violet momentum cutoff Λ used to regularize the otherwise ill-defined contact interactions in the Lagrangian—results in some of the nucleon-nucleon (NN) contact interactions being promoted to lower orders than they would appear according to NDA [19–21]. Similar effects occur in the so-called Pionless EFT, where the large nucleon-nucleon S-wave scattering lengths lead to shallow bound and virtual NN states that eventually give rise to relevant low-energy scales. These and other effects are reviewed in detail in Ref. [1].

* ajandis@ncsu.edu

† skoenig@ncsu.edu

Reference [22] extended the exploration of ChEFT with perturbative RG invariance to electromagnetic current operators by studying static properties (form factors) of the deuteron with use of perturbative RG-invariant chiral potentials developed in Refs. [23–25]. An important finding of this study is that, similar to what has been found for the chiral expansion of the nuclear interaction, the power counting for electromagnetic current operators in ChEFT needs to be modified, partially in line with the conclusion of a previous study based on the short-distance behavior of two-nucleon interacting wave function derived from the one-pion exchange (OPE) potential [26]. In this work, we extend this line of research to deuteron breakup, using deuteron electrodisintegration as a specific example. This inelastic reaction depends on both the initial deuteron bound state as well as on the continuum of neutron-proton final states, thus, by focusing on this process, we study a strictly larger range of physics than Ref. [22]. In particular, while the initial deuteron state is determined by the interaction in only the 3S_1 - 3D_1 coupled channels, the final-state interaction involves a number of other partial waves.

Direct calculation of dynamic observables for deuteron breakup is a feasible problem. However, such calculations of nuclear breakup reactions become increasingly difficult as the number of particles in the system increases. For this reason, we focus in this work on the Lorentz Integral Transform (LIT) method, first introduced in Ref. [27] and reviewed in Ref. [28]. The LIT makes it possible to perform breakup calculations with methods similar to those for bound states (albeit at the expense of working effectively with a complex energy), which enables *ab initio* many-body studies of such reactions for a range of atomic nuclei (see Ref. [29] and earlier references therein). A delicate inversion of the LIT is generally required to obtain the actual response function. Although it is not our main focus, we will review and refine an existing approach for inverting the LIT in order to obtain the response function. We also note that as an alternative to the LIT it has recently been suggested to work instead with integrated response functions, which can similarly be obtained with bound-state methods [30].

As a central part of this work, we derive the perturbative expansion of the LIT for a two-nucleon system, which is a crucial step towards studying nuclear breakup reaction with perturbatively renormalized EFTs. More precisely, in this approach, only leading order (LO) is treated nonperturbatively, with all corrections on top of that included in distorted-wave perturbation theory. This approach ensures that the EFT satisfies RG invariance at each order [1].

This paper is structured as follows. In Sec. II, we discuss in detail the theoretical framework for our calculation, including the LIT for the particular case of deuteron electrodisintegration and the perturbatively expanded, momentum-space representation. In this section we also briefly review the chiral interaction and current operators that we are using. Following this, we present selected re-

sults in Sec. III before we conclude with a summary and outlook in Sec. IV. Several more technical details are discussed in the appendix.

II. THEORETICAL FRAMEWORK

A. Response functions for electrodisintegration

We consider the process where an electron (e) scatters inelastically off a deuteron (d), breaking it up into its neutron (n) and proton (p) constituents. The cross section for this $d(e, e)np$ process can be written as [31–33]

$$\frac{d\sigma}{d\Omega d\omega} = \sigma_{\text{Mott}} \left[\frac{Q^4}{\mathbf{q}^4} \mathcal{R}_L(\omega, \mathbf{q}) + \left(\frac{Q^2}{2\mathbf{q}^2} + \tan \frac{\theta_e}{2} \right) \mathcal{R}_T(\omega, \mathbf{q}) \right], \quad (1)$$

where θ_e is the angle of the scattered electron and ω, \mathbf{q} are, respectively, the energy and three-momentum of a virtual space-like photon. Moreover, $Q^2 = -q_\mu^2 = \omega^2 - \mathbf{q}^2$ is the (positive) four-momentum transfer. Unless otherwise noted, we consider the energy and momentum components defined in the the c.m. frame of the outgoing nucleons. The prefactor σ_{Mott} in Eq. (1) is the Mott cross section and is given by

$$\sigma_{\text{Mott}} = \left(\frac{\alpha \cos \theta_e/2}{2E \sin^2 \theta_e/2} \right)^2, \quad (2)$$

with $\alpha \approx 1/137$ the electromagnetic fine-structure constant and E the initial electron energy ($\omega = E - E'$ with E' the energy of the scattered electron).

The objects $\mathcal{R}_L(\omega, \mathbf{q})$ and $\mathcal{R}_T(\omega, \mathbf{q})$ are the so-called longitudinal and transverse response functions, respectively, and they can be expressed in terms of nuclear matrix elements as follows:

$$\mathcal{R}_L(\omega, \mathbf{q}) = \frac{1}{3} \sum_{f \neq i} \sum_{m_i, m_f} |\langle \Psi_f | J_0 | \Psi_i \rangle|^2 \delta(\omega + E_i - E_f), \quad (3a)$$

$$\mathcal{R}_T(\omega, \mathbf{q}) = \frac{1}{3} \sum_{f \neq i} \sum_{m_i, m_f} \sum_{\lambda=\pm 1} |\langle \Psi_f | J_\lambda | \Psi_i \rangle|^2 \delta(\omega + E_i - E_f). \quad (3b)$$

In these expressions, $|\Psi_i\rangle$ represents the initial deuteron bound state and the $|\Psi_f\rangle$ are np final states with energy E_f , with total spin ($j_f = j_i = 1$) projections m_f (summed over) and m_i (averaged over), respectively.

¹ Following the literature on the subject, we have expressed \mathcal{R}_L and \mathcal{R}_T in terms of a *sum* over final states f , but it is understood that for transitions to continuum states (which for the deuteron without bound excited states is in fact the only possibility) this sum should strictly be an integral.

J_0 and J_λ are the charge-density and current operators in the one-photon-exchange approximation, respectively [31–33], which induce the transitions from initial to final states, and the delta functions in Eqs. (3) ensure conservation of energy. Elastic transitions ($f = i$) are explicitly excluded in the definitions of the response functions. For the remainder of this work, we will only consider the longitudinal response function because this already involves a significant fraction of the physics we are interested in, while avoiding the technical complexity of dealing with transverse current operators. We will also use the simpler notation $J_0 = \rho$ for the charge-density operator.

B. The Lorentz Integral Transform

The LIT of the longitudinal response function can be introduced as a convolution with a Lorentzian kernel [27, 28]:

$$\Phi(\sigma) = \int_{\omega_{\text{th}}}^{\infty} d\omega \tilde{\mathcal{R}}_L(\omega) L(\omega, \sigma). \quad (4)$$

Here σ is a complex parameter that in the following we mostly write out explicitly as $\sigma = \sigma_R + i\sigma_I$. The integral in Eq. (4) starts at the threshold energy ω_{th} , which is the transferred energy at which the breakup becomes possible, and extends up to infinity. The Lorentzian kernel is given by

$$L(\omega, \sigma) \equiv L(\omega, \sigma_R; \sigma_I) = \frac{1}{(\omega - \sigma_R)^2 + \sigma_I^2}, \quad (5)$$

and from this form it becomes obvious that Eq. (4) is indeed a convolution. The LIT $\Phi(\sigma) \equiv \Phi(\sigma_R; \sigma_I)$ is generally considered as a function of σ_R with a parametric dependence on σ_I that characterizes the “width,” *i.e.*, the resolution, of the transform.

Using this kernel, we now follow Martinelli *et al.* [34] (who performed an analogous derivation for three nucleons using the Faddeev formalism) and derive an abstract operator equation for the LIT. Inserting the definition of the longitudinal response function, Eq. (3a), into Eq. (4), averaging over the deuteron spin projection (as discussed

above), and summing over final states (including their spin projections m_f), gives

$$\Phi(\sigma_R; \sigma_I) = \frac{1}{3} \sum_{f \neq i} \sum_{m_i, m_f} \frac{|\langle \Psi_f | \rho | \Psi_i \rangle|^2}{\sigma_I^2 + (E_f - E_i - \sigma_R)^2}. \quad (6)$$

At this point, we expand the charge density operator into multipoles, writing²

$$\rho(\mathbf{q}) = \sum \sqrt{\hat{L}} \rho_L(q), \quad (7)$$

where the integer $L \geq 0$ denotes the multipole and $\hat{L} = 2L+1$. We use a coordinate system where the momentum \mathbf{q} of the photon is aligned along the z -axis and therefore there are no explicit spherical harmonics in Eq. (7) and the ρ_L appearing on the right-hand side are functions of $q = |\mathbf{q}|$ only; see Ref. [35] for more details. In general, by the Wigner-Eckart theorem, the multipole operators $\rho_L(q)$ between two nucleon states can be written as

$$\langle \Psi_f | \rho_L | \Psi_i \rangle = C_{j_f m_f, LM}^{j_i m_i} \langle \Psi_f | \rho_L | \Psi_i \rangle, \quad (8)$$

i.e., as a product of Clebsch-Gordan coefficients and reduced matrix elements. M here is the projection quantum number associated with L , and by our choice of coordinate system only $M = 0$ contributes; see Eqs. (B15) and (B31) in the Appendix for the precise expressions for the current operator that include these Clebsch-Gordan coefficients. Finally, while in principle the sum over L runs up to infinity, in practice one finds that convergence can be reached by truncating the sum at some $L = L_{\text{max}}$.

Inserting Eq. (8) into Eq. (6) allows us to explicitly evaluate the sum over spin projections of the squared matrix element:

$$\sum_{m_i, m_f} C_{j_f m_f, LM}^{j_i m_i} C_{j_f m_f, L' M'}^{j_i m_i} = \frac{2j_i + 1}{2L + 1} \delta_{LL'} \delta_{MM'}. \quad (9)$$

The numerator $2j_i + 1 = 3$ cancels against the $1/3$ from averaging, while the denominator can be canceled against the $\sqrt{\hat{L}\hat{L}'}$ arising from Eq. (7). Overall, we find

$$\Phi(\sigma_R; \sigma_I) = \sum_L \Phi_L(\sigma_R; \sigma_I), \quad (10)$$

and we can further rewrite each individual $\Phi_L(\sigma_R; \sigma_I)$:

² Note that our convention for the multipoles differs from the more

commonly used form for Coulomb multipoles (discussed, for example, in Ref. [35] (and *cf.* also Refs. [27, 36])) by a factor $\sqrt{4\pi} i^L$.

$$\begin{aligned}
\Phi_L(\sigma_R; \sigma_I) &= \sum_{f \neq i} \frac{|\langle \Psi_f | \rho_L | \Psi_i \rangle|^2}{\sigma_I^2 + (E_f - E_i - \sigma_R)^2} \\
&= \sum_{f \neq i} \frac{\langle \Psi_f | \rho_L | \Psi_i \rangle \langle \Psi_i | \rho_L^\dagger | \Psi_f \rangle}{(E_f - E_i - \sigma_R + i\sigma_I)(E_f - E_i - \sigma_R - i\sigma_I)} \\
&= \sum_{f \neq i} \langle \Psi_i | \rho_L^\dagger (H - E_i - \sigma_R - i\sigma_I)^{-1} | \Psi_f \rangle \langle \Psi_f | (H - E_i - \sigma_R + i\sigma_I)^{-1} \rho_L | \Psi_i \rangle.
\end{aligned} \tag{11}$$

In the last line we have used the fact that the final states satisfy the Schrödinger equation $H|\Psi_f\rangle = E_f|\Psi_f\rangle$, and we swapped the order of the matrix elements to make the following steps more obvious. Finally, we note that of course there is a multipole expansion like Eq. (10) directly for the response function, and Eq. (11) can be obtained from applying the LIT (4) separately to each term in that expansion.

In the last line of Eq. (11), the sum runs over all possible final states *except* $|\Psi_i\rangle$, *i.e.*, the ground-to-ground state transition is explicitly excluded. Further following Ref. [34], we can extend the sum to include this term and subtract it at the end to compensate, noting that it can be written in terms of the elastic form factor. This allows us to identify the sum over all final states with the identity, by means of completeness, and to arrive at

$$\Phi_L(\sigma_I, \sigma_R) = \langle \Psi_i | \rho_L^\dagger (H - E_i - \sigma_R - i\sigma_I)^{-1} (H - E_i - \sigma_R + i\sigma_I)^{-1} \rho_L | \Psi_i \rangle - \frac{|\langle \Psi_i | \rho_L | \Psi_i \rangle|^2}{\sigma_R^2 + \sigma_I^2}, \tag{12}$$

From this form one can see that the first term in Eq. (11) can be written as the squared norm of a state $|\Phi_i\rangle$ that satisfies the LIT equation

$$(H - E_i - \sigma_R + i\sigma_I) |\Phi_L\rangle = \rho_L |\Psi_i\rangle, \tag{13}$$

where ρ_L is understood to ultimately yield a reduced matrix element, *i.e.*, the Clebsch-Gordan coefficient from the charge density operator has already been eliminated by summing over the total spin projections, as discussed above. This equation is similar to the Schrödinger equation with an inhomogeneous source term and a shifted, complex energy. We can ultimately express the LIT for multipole L as

$$\Phi_L(\sigma_R; \sigma_I) = \langle \Phi_L | \Phi_L \rangle - |\langle \Psi_i | \Phi_L \rangle|^2, \tag{14}$$

where we have used a convenient alternative form for the second term in Eq. (12) [34], which we refer to as the “elastic term.” For $L = 0$, it is proportional to the square of the deuteron form factor, and therefore the alternative form in Eq. (14), which follows directly from Eq. (13) by noting that $|\Psi_i\rangle$ is an eigenstate of H with energy E_i , can also be used to test the LIT numerics against a direct evaluation of the form factor; this is discussed further in Sec. III A.

The source term on the right-hand side of Eq. (13) determines the asymptotic behavior of the solution and is the key to understanding many features of the LIT. In particular, together with the explicit imaginary part added to the energy, it imposes a boundary condition that ensures that $|\Phi_{m_i}\rangle$, when expressed in coordinate space, exhibits an exponentially decaying tail, just like

the initial bound state. In other words, these features of the equation ensure that $\langle \Phi | \Phi \rangle$ is well defined and finite.

Moreover, we can write $H = H_0 + V$ with the free Hamiltonian H_0 and rewrite Eq. (13) as

$$(H_0 - E_i - \sigma^*) |\Phi_{m_i}\rangle + V |\Phi\rangle = \rho |\Psi_{m_i}\rangle \tag{15a}$$

$$\implies (G_0 V - 1) |\Phi_{m_i}\rangle = G_0 \rho |\Psi_{m_i}\rangle, \tag{15b}$$

where $G_0 = G_0(E_i + \sigma^*) = (H_0 - E_i - \sigma^*)^{-1}$ is the free Green’s function evaluated at a complex energy $E_i + \sigma^*$. The combination of operators on the left-hand side of Eq. (13) is exactly what otherwise appears, for real energies, in the Lippmann-Schwinger equation that defines the continuum scattering states.

C. Partial-wave expansion

In addition to using the multipole expansion for the current operator, we also project all equations into momentum-space partial waves. For this, we write as $|p; \alpha\rangle = |p\rangle \otimes |\alpha\rangle$ with p the NN center-of-mass momentum and $|\alpha\rangle = |(ls)j, t\rangle$ collecting the spin and isospin quantum numbers. We will in the following often use standard spectroscopic notation to identify particular spin/isospin channels. We furthermore use conventions in which the completeness relation reads

$$1 = \sum_{\alpha} \int dp p^2 |p; \alpha\rangle \langle p; \alpha|. \tag{16}$$

Equation (15b) is straightforward to project into this space, using Eq. (16) and the fact that G_0 is diagonal in

both momentum and α . The momentum-space partial-wave representation of the charge-density operator multipoles, which will be introduced in more detail in Sec. II E, is discussed in Appendix B. After discretizing all momenta on a quadrature mesh, Eq. (15b) ultimately becomes an inhomogeneous linear matrix-vector equation, which is solved with standard techniques.

In the following, we will suppress the explicit L subscript for $|\Phi\rangle$, noting that in our numerical calculation, we solve a LIT matrix-vector equation of the form (15b) for each L and ultimately sum over L , as discussed in Sec. II B. The channels α in which $|\Phi\rangle$ has nonzero components depend on the multipole L and on the current operator. Different operators enter at different orders in the EFT expansion, which in fact has to be applied to the LIT formalism overall. This is the topic of the following subsections.

D. Perturbative expansion

The EFT expansion gives rise to a series of potentials,

$$V = V^{(0)} + V^{(1)} + V^{(2)} + \dots, \quad (17)$$

where $V^{(0)}$ is the LO potential that is treated nonperturbatively, and $V^{(i)}$ with $i \geq 1$ are perturbative corrections. Importantly, this expansion is to be propagated strictly to all observables to maintain a properly renormalized theory. For example, the energy of the initial state has an expansion of the form

$$E_i = E_i^{(0)} + E_i^{(1)} + E_i^{(2)} + \dots, \quad (18)$$

which follows directly from the expansion of the deuteron binding energy, $B = B^{(0)} + B^{(1)} + B^{(2)} + \dots$, since $E_i = -B$; see Appendix A for details.

We are interested in the perturbative expansion of the LIT of the form

$$\Phi_L(\sigma) = \Phi_L(\sigma)^{(0)} + \Phi_L(\sigma)^{(1)} + \Phi_L(\sigma)^{(2)} + \dots. \quad (19)$$

All equations in this section are valid for a fixed multipole L and it is understood that multipole contributions are ultimately to be summed according to Eq. (10). To keep the notation simple, we omit the explicit multipole subscript L in the following.

To obtain the higher-order corrections to the LIT, we

expand $|\Phi\rangle = |\Phi_L\rangle$ and $|\Psi\rangle$ in the following way

$$|\Phi\rangle = |\Phi^{(0)}\rangle + |\Phi^{(1)}\rangle + |\Phi^{(2)}\rangle + \dots, \quad (20)$$

$$|\Psi\rangle = |\Psi^{(0)}\rangle + |\Psi^{(1)}\rangle + |\Psi^{(2)}\rangle + \dots, \quad (21)$$

where the latter is the standard perturbative expansion of the deuteron bound state, reviewed briefly in Appendix A.

Inserting these expansions into Eq. (14) leads to two different kinds of overlaps, which we denote as \mathcal{A} and \mathcal{B} . Up to second-order, their perturbative expansions are

$$\mathcal{A}^{(0)} = \langle \Phi^{(0)} | \Phi^{(0)} \rangle, \quad (22a)$$

$$\mathcal{A}^{(1)} = \langle \Phi^{(0)} | \Phi^{(1)} \rangle + \langle \Phi^{(1)} | \Phi^{(0)} \rangle, \quad (22b)$$

$$\mathcal{A}^{(2)} = \langle \Phi^{(1)} | \Phi^{(1)} \rangle + \langle \Phi^{(0)} | \Phi^{(2)} \rangle + \langle \Phi^{(2)} | \Phi^{(0)} \rangle, \quad (22c)$$

and

$$\mathcal{B}^{(0)} = \langle \Psi^{(0)} | \Phi^{(0)} \rangle, \quad (23a)$$

$$\mathcal{B}^{(1)} = \langle \Psi^{(0)} | \Phi^{(1)} \rangle + \langle \Psi^{(1)} | \Phi^{(0)} \rangle, \quad (23b)$$

$$\mathcal{B}^{(2)} = \langle \Psi^{(1)} | \Phi^{(1)} \rangle + \langle \Psi^{(0)} | \Phi^{(2)} \rangle + \langle \Psi^{(2)} | \Phi^{(0)} \rangle, \quad (23c)$$

Using these, we can now express the desired perturbative expansion of the LIT as

$$\Phi(\sigma)^{(0)} = \mathcal{A}^{(0)} - |\mathcal{B}^{(0)}|^2, \quad (24a)$$

$$\Phi(\sigma)^{(1)} = \mathcal{A}^{(1)} - \mathcal{B}^{(0)} \mathcal{B}^{(1)*} - \mathcal{B}^{(1)} \mathcal{B}^{(0)*}, \quad (24b)$$

$$\Phi(\sigma)^{(2)} = \mathcal{A}^{(2)} - |\mathcal{B}^{(1)}|^2 - \mathcal{B}^{(0)} \mathcal{B}^{(2)*} - \mathcal{B}^{(2)} \mathcal{B}^{(0)*}. \quad (24c)$$

While the expansion of the deuteron state $|\Psi\rangle$ is well known, we need to derive the equations that determine the perturbative components $\Phi^{(0)}$, $\Phi^{(1)}$, and $\Phi^{(2)}$ of the LIT state. This is achieved by systematically expanding all quantities in Eq. (15b), which includes the perturbative expansion of the charge-density operator ρ :

$$\rho = \rho^{(0)} + \rho^{(1)} + \rho^{(2)} + \dots. \quad (25)$$

Along with the expansion of the free Green's function (which follows directly from the expansion of the initial energy),

$$G_0 = G_0 - E_i^{(1)} G_0^2 - [E_i^{(1)}]^2 G_0^3 - E_i^{(2)} G_0^2 + \dots, \quad (26)$$

we obtain altogether:

$$(G_0 V^{(0)} - 1) |\Phi^{(0)}\rangle = G_0 \rho^{(0)} |\Psi_i^{(0)}\rangle, \quad (27a)$$

$$(G_0 V^{(0)} - 1) |\Phi^{(1)}\rangle = G_0 (E_i^{(1)} - V^{(1)}) |\Phi^{(0)}\rangle + G_0 [\rho^{(1)} |\Psi_i^{(0)}\rangle + \rho^{(0)} |\Psi_i^{(1)}\rangle], \quad (27b)$$

$$\begin{aligned} (G_0 V^{(0)} - 1) |\Phi^{(2)}\rangle &= G_0 (E_i^{(2)} - V^{(2)}) |\Phi^{(0)}\rangle + G_0 (E_i^{(1)} - V^{(1)}) |\Phi^{(1)}\rangle \\ &\quad + G_0 [\rho^{(2)} |\Psi_i^{(0)}\rangle + \rho^{(0)} |\Psi_i^{(2)}\rangle + \rho^{(1)} |\Psi_i^{(1)}\rangle]. \end{aligned} \quad (27c)$$

Written in this way, we can see that at each order in the perturbative expansion, the LIT equations share the same “kernel operator” ($G_0 V^{(0)} - 1$) and only differ in their inhomogeneous terms. These inhomogeneous terms involve the lower-order LIT amplitudes, so ultimately we have a scheme that can be evaluated sequentially.

E. Chiral interaction

We follow the power counting developed in Refs. [23–25] for the chiral potentials, and in Ref. [22] for the electric charge operators. For completeness, we explain briefly here how these nuclear forces are arranged.

Generally, the potential derived from CheFT at a given order receives contributions from pion exchanges between the nucleons, as well as from contact interactions that parameterize unresolved short-distance physics. The expressions for pion-exchange potentials have become standardized and we use Ref. [37] for the one-pion exchange (OPE) and the leading two-pion exchange (TPE) potentials, *i.e.*, Feynman diagrams made up of vertices with chiral index $\nu = 0$, referred to as “TPE0” in Ref. [37]. One-pion exchange provides the longest-range component of the nuclear force.³ The values of the various parameters adopted here include the nucleon axial coupling constant $g_A = 1.29$, the pion decay constant $f_\pi = 92.4$ MeV, the pion mass $m_\pi = 138$ MeV, and the average nucleon mass $m_N = 939$ MeV.

By definition, all LO forces are nonperturbative, *i.e.*, they need to be fully iterated by solving the Schrödinger or Lippmann-Schwinger equations. In line with this, the LIT expansion discussed in the previous section treats $V^{(0)}$ nonperturbatively.

The OPE potential contributes to all NN partial waves. While it can be strongly attractive in some of these channels, as angular momentum l increases between

the two nucleons the OPE potential is gradually weakened by the centrifugal barrier and therefore becomes perturbative. Following Refs. [25, 39], we choose 1S_0 , 3S_1 - 3D_1 , and 3P_0 to be the channels where OPE must be at LO, and in each of these channels there is a contact potential, also referred to as a counterterm in the literature, at this order. For the S waves, these contact potentials would anyway enter at LO, while for 3P_0 NDA alone would suggest that the P -wave contact only enters as a higher-order correction. For each channel where OPE is attractive and singular, the Schrödinger equation does not have a well-defined solution without an ultra-violet regularization, even though the OPE potential itself is well-defined [40]. A counterterm needs to be included in each of these channels if one chooses the potential to enter at LO [19]. Each of the contact terms discussed below are determined at the order in which they appear via fitting to the empirical phase shifts for the corresponding partial wave, provided by the Nijmegen partial-wave analysis [41, 42], up to $k = 300$ MeV where k is the center-of-mass momentum.

In the 1S_0 and 3S_1 channels, the short-range, contact potentials V_S at LO have the form

$$\langle p'; \alpha | V_S^{(0)} | p; \alpha \rangle = C_0^{(0)} \quad (28)$$

where α represents a given partial wave and p (p') is the incoming (outgoing) relative momentum, as introduced in Sec. II C. We use the “(0)” superscript to indicate LO potentials and LECs, as done for other quantities in Sec. II D. As the contact potentials are formulated directly in the partial-wave basis, we omit the channel subscript α on the LECs when there is no ambiguity. In 3P_0 , the contact potential features an explicit momentum dependence in accordance with a generic P -wave short-range interaction:

$$\langle p'; ^3P_0 | V_S^{(0)} | p; ^3P_0 \rangle = C_0^{(0)} p' p. \quad (29)$$

In all other channels, the LO potential vanishes in the power counting of Refs. [25].

At next-to-leading order (NLO), OPE enters in the channels where it is considered perturbative. Following further Refs. [23–25], we include OPE in all partial waves with orbital angular momentum $l \leq 2$, and those coupled to them, 3F_2 and 3G_3 , deeming OPE in yet higher partial waves to be negligible. The cutoff on l is chosen

³ Electromagnetic forces behave like a power law at large distances and therefore have a strictly longer range than OPE. It is customary to consider these separate from the “strong” nuclear force, although in fact the two cannot be strictly separated, see *e.g.* Ref. [38]. In any case, we do not need to consider electromagnetic forces between the neutron and the proton in this work to the order we are working at.

rather empirically, based on the observation that the F -wave phases shifts in the partial-wave analysis, *e.g.*, of Ref. [42] are mostly $\lesssim 2^\circ$. We note that this choice is in line with Ref. [43], where OPE is counted as next-to-next-to-next-to-leading order (N3LO) in the spin-singlet channels, and we stop at next-to-next-to-leading order (N2LO) in this paper. Unfortunately, similar analyses on the triplet channels are not yet available. In addition, the 1S_0 contact potential receives a momentum-dependent correction at NLO [24]:

$$\langle p'; ^1S_0 | V_S^{(1)} | p; ^1S_0 \rangle = C_0^{(1)} + \frac{D_0^{(1)}}{2} (p'^2 + p^2), \quad (30)$$

where $C_0^{(1)}$ is the NLO correction to the LO LEC $C_0^{(0)}$ and $D_0^{(1)}$ is the LEC associated with the momentum-dependent 1S_0 contact interaction (which would naively enter at N2LO).

At N2LO, TPE0 enters in the channels where OPE enters at LO (*i.e.*, 1S_0 , 3S_1 – 3D_1 , and 3P_0), while in other channels two-pion exchange enters at higher order. For the short-range potentials in these channels, the power counting gives the following contributions at N2LO:

$$\langle p'; ^1S_0 | V_S^{(2)} | p; ^1S_0 \rangle = E_0^{(2)} p'^2 p^2, \quad (31a)$$

$$\langle p'; ^3S_1 | V_S^{(2)} | p; ^3S_1 \rangle = C_0^{(2)} + \frac{D_0^{(2)}}{2} (p'^2 + p^2), \quad (31b)$$

$$\langle p'; ^3D_1 | V_S^{(2)} | p; ^3S_1 \rangle = E_0^{(2)} p'^2. \quad (31c)$$

In the channels where OPE is perturbative, we have the following P -wave contact potentials at N2LO:

$$\langle p'; ^1P_1 | V_S^{(2)} | p; ^1P_1 \rangle = C_0^{(2)} p' p, \quad (32a)$$

$$\langle p'; ^3P_1 | V_S^{(2)} | p; ^3P_1 \rangle = C_0^{(2)} p' p, \quad (32b)$$

$$\langle p'; ^3P_2 | V_S^{(2)} | p; ^3P_2 \rangle = C_0^{(2)} p' p. \quad (32c)$$

In practical calculations, all interactions are regularized using a momentum cutoff Λ , with $\Lambda \rightarrow \infty$ corresponding to the zero-range limit. We implement this cutoff regularization in a separable manner, *i.e.*, we have, generically,

$$\langle \alpha p' | V_\Lambda | \alpha p \rangle \sim g(p') [\dots] g(p), \quad (33)$$

where $[\dots]$ represents the zero-range expression for the potential and $g(p) = \exp(-p^4/\Lambda^4)$.

F. Current operator

1. Overview

At LO, the charge density is given by a simple one-body operator that describes a photon coupling to the nucleon charge:

$$\begin{aligned} \rho^{(0)}(\mathbf{q}; \mathbf{p}, \mathbf{p}') &= \langle \mathbf{p} | \rho^{(0)}(\mathbf{q}) | \mathbf{p}' \rangle = e \frac{1 + \tau_3^{(1)}}{2} \\ &\times \delta^{(3)}\left(\mathbf{p} - \mathbf{p}' - \frac{\mathbf{q}}{2}\right) + 1 \rightleftharpoons 2, \quad (34) \end{aligned}$$

There is no NLO correction to the charge-density operator, but at N2LO, two corrections enter. Following Refs. [12, 22, 44], we write these as

$$\begin{aligned} \rho_{\text{rel}}^{(2)}(\mathbf{q}; \mathbf{p}, \mathbf{p}') &= -\frac{e}{8M_N^2} \left(\frac{1}{2} + \kappa_s + \left(\frac{1}{2} + \kappa_v \right) \tau_3^{(1)} \right) \\ &\times \left(q^2 + 2i\mathbf{q} \cdot \boldsymbol{\sigma}_1 \times \mathbf{K} \right) \delta^{(3)}\left(\mathbf{p} - \mathbf{p}' - \frac{\mathbf{q}}{2}\right) + 1 \rightleftharpoons 2 \quad (35a) \end{aligned}$$

and

$$\rho_{\text{str}}^{(2)}(\mathbf{q}; \mathbf{p}, \mathbf{p}') = -\frac{e}{6} \langle r_s^2 \rangle q^2 \delta^{(3)}\left(\mathbf{p} - \mathbf{p}' - \frac{\mathbf{q}}{2}\right), \quad (35b)$$

where $\kappa_s(\kappa_v)$ and r_s are, respectively, the isoscalar (isovector) anomalous magnetic moment and the isoscalar charge radius of the nucleon. We have written Eqs. (34) and (35a) in terms of nucleon “1” being struck by the photon, with “1 \rightleftharpoons 2” indicating that there is an analogous term to be added with superscript “(2)” on the isospin operator τ_3 ; for the deuteron system that we consider here, both terms ultimately give the same result and we account for this with a factor two in our implementation. Moreover, $\mathbf{K} = \mathbf{p}/2 + \mathbf{p}'/2 - \mathbf{q}/4$ in the c.m. frame of the outgoing nucleons that we are working in.

2. Relativistic considerations

All the operators described above are defined in the two-nucleon c.m. frame, and the expressions we have given follow from specializing the generic expressions of Ref. [12] to this frame by inserting the appropriate expressions for the kinematic variables. One thing to note in this regard is that the resulting expressions for the operators turn out to be formally the same as those for the form-factor calculations in Ref. [22], even though that analysis is performed in the so-called “Breit frame,” defined by the virtual photon transferring only momentum and no energy to the deuteron. One notable difference is that in the Breit frame, $\mathbf{K} = \mathbf{p} + \mathbf{q}/4$. Seemingly, this would change the expression for $\rho_{\text{rel}}^{(2)}(\mathbf{q}; \mathbf{p}, \mathbf{p}')$ in Eq. (35a). However, by using the identity

$$\mathbf{q} \cdot \boldsymbol{\sigma}_1 \times \mathbf{K} = \boldsymbol{\sigma}_1 \cdot \mathbf{K} \times \mathbf{q}, \quad (36)$$

it becomes evident that any terms proportional to \mathbf{q} in \mathbf{K} drop out, and then by means of overall momentum conservation one can easily transform the Breit-frame expression into the c.m.-frame one.

While the three-momentum transfer \mathbf{q} is in principle a frame-dependent quantity, it is important to note that $q = |\mathbf{q}|$ can be consistently (*i.e.*, up to differences that are of higher order than we work at in the EFT power counting) assumed to be the same in both frames referred to above. Accordingly, the discussion above is already exploiting this observation in simply referring to the momentum transfer as \mathbf{q} , without indication which frame it should refer to. The argument for this equivalence goes as follows:

1. In the c.m. frame, the outgoing neutron-proton pair is at rest, whereas prior to the reaction the deuteron moves with momentum $-\mathbf{q}$. In the Breit frame, on the other hand, the deuteron moves with momentum $-\mathbf{q}/2$ before being struck by the photon, and with momentum $\mathbf{q}/2$ afterwards. The relative motion between the two frames is pointing along the z -axis and can be written as $\beta = \Delta v/c = (v_{\text{c.m.}} - v_{\text{Breit}})/c$, where $c = 1$ in our conventions. Then, with $\mathbf{q} = M_d \mathbf{v}$ (where $M_d = 2M_N - B_d$ the deuteron mass), we can write

$$\beta = \frac{\Delta q}{M_d} = \mathcal{O}(1/M_N). \quad (37)$$

2. A boost from the Breit frame to the c.m. frame simply amounts to $q \rightarrow \gamma q$ with $\gamma \approx 1 + \beta^2/2$. In principle there is another term $-\beta\gamma\omega$, but this vanishes identically if we start in the Breit frame, and it is otherwise suppressed by another factor $\beta \sim 1/M_N$. Using $\beta = \mathcal{O}(1/M_N)$ as determined above, we find that the net change is of order $1/M_N^2$, *i.e.*, it is of the same order as the explicit relativistic correction to the current, Eq. (35a), which we include specialized to the c.m. frame.
3. Considering that $Q^2 = -q_\mu q^\mu = \mathbf{q}^2 - \omega^2$ is the Lorentz-invariant squared four-momentum transfer, and ω being an explicit parameter in the c.m. frame (that in fact we use to define the response function and LIT), it might seem odd to write the contribution $\rho_{\text{str}}^{(2)}$ given in Eq. (35b) in terms of q^2 only, when generally it should feature Q^2 [44]. However, by the above analysis it is indeed consistent to formally count $\omega \sim \mathbf{q}^2/M_N$, and to consequently take $Q^2 = q^2 = \mathbf{q}^2$ as the same in all frames—up to corrections of order $1/M_N^2$ (see also Ref. [45] for this conclusion).

3. Boost correction

One further correction to consider arises from the fact that we perform the LIT calculation in the c.m. frame of the outgoing nucleons, which, as already mentioned, before the collision is the frame that moves with total momentum $-\mathbf{q}$, while calculation of the bound-state wave function we use in this work (and that is standard) assumes the deuteron is at rest (*i.e.*, effectively, in the laboratory frame). Consistency requires that this wave function before the collision must be boosted into the c.m. frame, and, according to the EFT power counting discussed below, this boost correction enters at N2LO.

The boost correction has already been studied in detail for calculations of the deuteron form factors [22, 44, 46]. In that case, the situation is slightly different compared to the breakup process because, as already mentioned in the previous section, form factors are typically calculated in the Breit frame. In the form-factor matrix

element $\langle \Psi | \mathcal{O} | \Psi \rangle$, where \mathcal{O} denotes a generic current operator, the ket-side deuteron then moves with momentum $-\mathbf{q}/2$ whereas the bra-side deuteron moves with momentum $+\mathbf{q}/2$. In this situation, boosts are required for the deuteron states on both sides if their wave functions are calculated in the rest frame.

While in general the Lorentz boost operator acting on a deuteron state is quite complicated (due to the deuteron being a spin-1 particle), it has been shown in Ref. [46] that for the form-factor calculation the boost effect can be reduced to merely a relativistic rescaling of the longitudinal argument of the deuteron wave function expressed in momentum space (see Ref. [22] for a recent application of this). The key to being able to perform this simplification is that spin-1 states appear on both sides of the form-factor matrix element, while the relevant current operators are odd functions under spin exchange [46]. For the breakup calculation we consider here, this remains true for the leading current operator $\rho^{(0)}$, which we shall see is the only current operator that enters together with the boost up to N2LO in the power counting. Specifically, if we look at the explicit expression for the longitudinal response function, Eq. (3a), we have matrix elements of the form $\langle \Psi_f | \rho^{(0)} | \Psi_i \rangle$ in which $|\Psi_i\rangle$ needs to be boosted. Both $|\Psi_i\rangle$ and $|\Psi_f\rangle$ are $S = 1$ states because $\rho^{(0)}$ does not flip a nucleon spin, and therefore the situation is the same as for the form-factor calculation.

The calculation of the boost correction as outlined above leads to expressions of the form

$$\langle \mathbf{p} | \rho^{(0)} | \Psi_{i,\eta} \rangle = \Psi_i \left(\mathbf{p} + \frac{\mathbf{q}}{2\sqrt{1+\eta}} \right), \quad (38)$$

where $\eta = q^2/(4M_N^2)$ describes the relativistic boost from the deuteron rest frame to the c.m. frame (cf. the discussion in Sec. II F 2), and $|\Psi_{i,\eta}\rangle$ is the boosted deuteron state. We have explicitly used here that the LO current $\rho^{(0)}$ amounts to merely evaluating at a shifted momentum, and only this shift becomes modified by the relativistic boost per the discussion above. This ultimately allows us to model the boost correction, although strictly it arises from the deuteron wave function, as an *effective current correction*. That is, we can expand Eq. (38) to first order in $\eta \sim Q^2/M_N^2$ to isolate the N2LO effect, and then construct an N2LO operator $\rho_{\text{boost}}^{(2)}$ that, when applied to $|\Psi_i\rangle$, reproduces the same expression.

One can obtain an expression for this operator from the aforementioned expansion of the charge density into multipoles in a partial-wave momentum basis. As detailed in Appendix B 1, the (spin-decoupled) spatial part of the matrix element of $\rho^{(0)}$ can be written in the form

$$\begin{aligned} \langle u; lm | \tilde{\rho}^{(0)}(\mathbf{q}) | u'; l'm' \rangle &= \sum_L \sqrt{\hat{L}} C_{lm,L0}^{l'm'} \\ &\times \int_{-1}^1 dx G_{l,l'}^L(u, q, x) \frac{\delta(u' - \iota(u, q, x))}{u'^2}, \end{aligned} \quad (39)$$

where the function $G_{l,l'}^L(u, q, x)$ is defined in Eq. (B14) and $\iota(u, q, x) = \sqrt{p^2 - p q x + q^2/4}$, as defined also in Eq. (B25). To isolate the N2LO boost correction, we need to apply the substitution

$$q \rightarrow \frac{q}{\sqrt{1+\eta}} \quad (40)$$

in Eq. (39) and then Taylor-expand the resulting expression to first order. We see from this there arises two distinct terms: one from the q dependence of $G_{l,l'}^L(u, q, x)$ and another from the $\iota(u, q, x)$ inside the Dirac delta function. The latter gives a term proportional to $\delta'(u' - \iota(u, q, x))$, which, when the operator is applied to a state, ultimately leads to a first-order derivative of the momentum-space deuteron wave function. Overall, the detailed expressions for the matrix elements of the effective current operator $\rho_{\text{boost}}^{(2)}(\mathbf{q})$ are given in Appendix B 3. To conclude this discussion, we note that the formalism described here can also describe the boost required for the form-factor calculation, one merely needs to make the replacement $\eta \rightarrow \eta_{\text{Breit}} = q^2/(4M_d^2)$ to arrive at the expression given in Refs. [22, 44, 46].

III. RESULTS

A. Sanity checks

As explained in Sec. II B, for $L = 0$ the second term in Eq. (12) is proportional to the square of the deuteron elastic charge form factor, which can be calculated as

$$F_C(q^2) = \langle \Psi | \rho_0 | \Psi \rangle. \quad (41)$$

Using $H|\Psi\rangle = E_i|\Psi\rangle$ along with

$$|\Phi_0\rangle = (H - E_i - \sigma_R + i\sigma_I)^{-1} \rho_0 |\Psi\rangle \quad (42)$$

yields

$$\langle \Psi | \Phi_0 \rangle = \frac{\langle \Psi | \rho_0 | \Psi \rangle}{-\sigma_R + i\sigma_I}, \quad (43)$$

which is what leads to Eq. (14).

This relation provides an excellent opportunity to check, numerically, the LIT states $|\Phi\rangle$ against a direct calculation of $F_C(q^2)$. Moreover, this comparison against a direct evaluation of the form factor can be performed perturbatively at each order. Obtaining a consistent form factor from $\langle \Psi | \Phi \rangle$ is a necessary (although not sufficient) criterion for $|\Phi\rangle$ to be calculated correctly. Making use of our notation from Sec. II D, this leads to

$$F_C^{(n)} = (-\sigma_R + \sigma_I) \mathcal{B}^{(n)} \quad (44)$$

for all orders n .

However, as discussed in Sec. II F, at N2LO ($n = 2$) one needs to take into account relativistic corrections, and

carefully consider the frame in which the expressions are defined. Per the discussion in Sec. II F 2, all genuine current operators at this order are formally the same in the Breit frame (the standard choice for calculating the form factor) and the c.m. frame (used to calculate the LIT of the longitudinal response function that describes the breakup process). However, the boost correction detailed in Sec. II F 3 *does* depend on the frame, and therefore the direct equivalence breaks at this point.

As we are merely looking to check our numerical implementation, we perform the following comparison with the boost correction disabled at N2LO. We have independently verified that our direct calculation of the form factor, using Eq. (41), perturbatively expanded, agrees well with the calculation of Shi *et al.* [22]. There is no NLO column in the table because there is no NLO correction to the form factor: such a correction would be generated only by an NLO contribution to the 3S_1 - 3D_1 potential or by an NLO current operator, both of which are absent. For the LIT calculations (shown in the following section), there *are* NLO corrections that stem from the NLO 1S_0 potential contribution.

B. Convergence studies

In this section, we study how the LIT of the deuteron longitudinal response function converges with respect to the order of the chiral expansion, and at each order we also verify that the calculation converges as the momentum cutoff Λ increases, indicating that the theory is properly renormalized. The Chiral EFT interaction that we are using has been shown to describe well both two-nucleon scattering and deuteron form factors, and to converge for these observables in the sense mentioned above, but for the electrodisintegration process we are studying here, this still needs to be tested explicitly.

In Fig. 1 we show a comparison of the LIT calculated at different EFT orders, including corrections to both the potential as well as to the current operator (as discussed in Sec. II E). At each order, we show results for several cutoffs Λ . For these calculations, which use $\mathbf{q}^2 = 0.6 \text{ MeV}^2$ for the momentum transfer and set $\sigma_I = 3.0 \text{ MeV}$ for the LIT. We find good convergence with the cutoff, with very little variation beyond $\Lambda = 600 \text{ MeV}$. In Fig. 2, we show the same data as in Fig. 1 in a different form, comparing the different EFT orders at a fixed EFT cutoff value $\Lambda = 800 \text{ MeV}$, just to further illustrate our findings.

Convergence with respect to the order-by-order EFT expansion is a bit more difficult to interpret, and we note that the LIT at NLO is very close to the LO result. The reason for this is that, in the power-counting scheme we are using, at NLO there are corrections only to the potential, namely a short-range contact term in the 1S_0 channel, as well as OPE in the channels where it did not enter already at LO. In particular, there are no potential corrections in the 3S_1 - 3D_1 channel (and thus no correc-

$q^2 (m_\pi)$	LIT (LO)	direct (LO)	LIT (N2LO*)	direct (N2LO*)
0.5	0.92888	0.92888	-0.01018	-0.01018
1	0.76810	0.76809	-0.03394	-0.03394
2	0.59589	0.59588	-0.05975	-0.05976
3	0.44786	0.44785	-0.08043	-0.08043
4	0.23935	0.23935	-0.09774	-0.09774
5	0.11748	0.11747	-0.08590	-0.08591
6	0.04836	0.04836	-0.05578	-0.05580

Table I. Form factors extracted from the LIT calculation compared to a direct evaluation. As discussed in the text, the boost correction that enters at N2LO differs between the LIT and a direct form-factor calculation. The values in the table therefore omit the boost correction at N2LO, indicated with an asterisk.

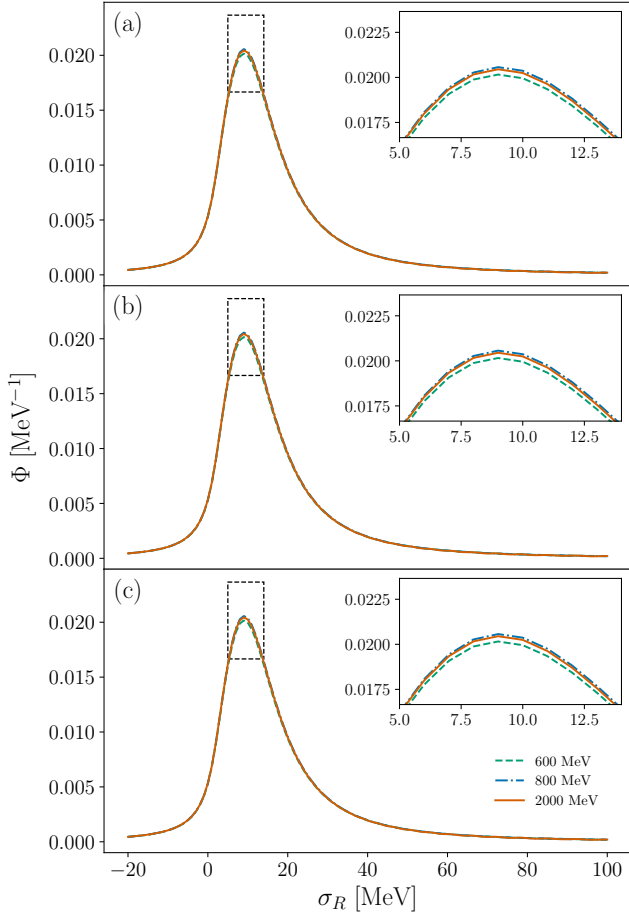


Figure 1. LIT of the deuteron longitudinal response for $q^2 = 0.6 \text{ fm}^{-2}$, $\sigma_I = 3.0 \text{ MeV}$ at (a) LO (b) NLO and (c) N2LO. Each panel shows the LIT for three different values of the momentum cutoff Λ .

tions to the deuteron wave function) or to the current (charge density) operator at this order. For the LIT of the longitudinal response, these potential corrections *do* play a role, but the effect of this final-state interaction⁴

⁴ In a direct calculation of the response function, it becomes more

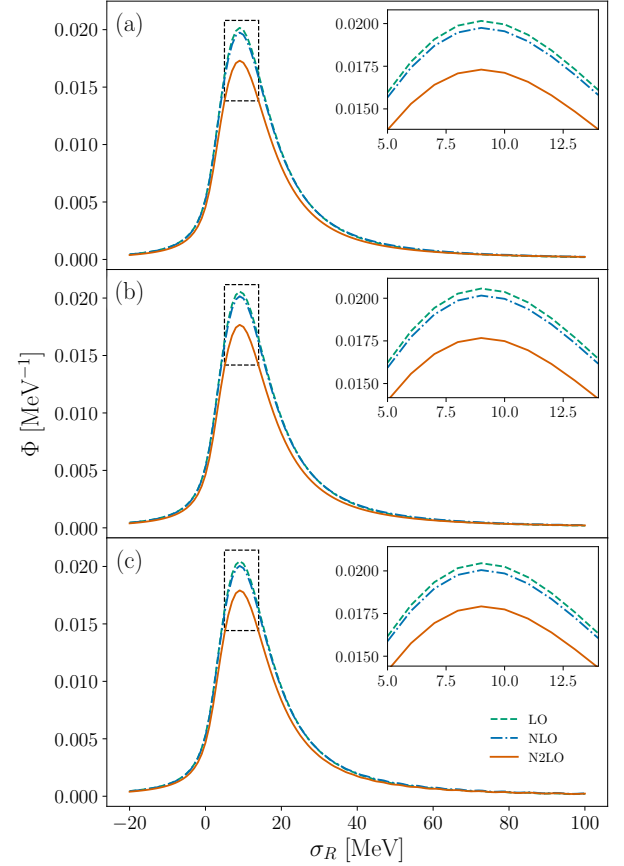


Figure 2. LIT of the deuteron longitudinal response at different orders for $\sigma_I = 3.0 \text{ MeV}$, $q^2 = 0.5 \text{ fm}^{-2}$.

is suppressed in the kinematic region of the quasi-elastic peak (see, for example, Refs. [47, 48] for discussions of this), and therefore not very pronounced in our plotted results. If one studies the NLO correction relative to LO, then indeed as one moves away from the peak (*e.g.*, by

obvious that there is a correction at NLO to only the “final-state interaction” between the proton and neutron arising from the deuteron breaking up.

increasing σ_R at fixed q^2), one can see that the NLO correction becomes more sizable.

At N2LO, there are corrections to the potential in various channels, and, as discussed in Sec. II E, also to the current operator. Overall these effects combine to decrease the magnitude of the LIT, which is particularly notable in the peak region. At this order, there is a bit more spread as the cutoff is varied, but overall we still observe rapid convergence with increasing Λ .

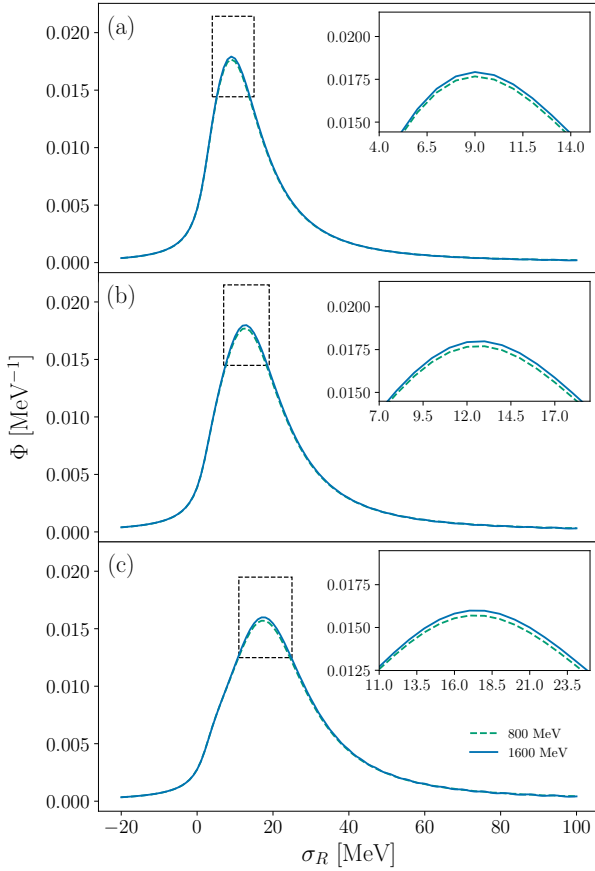


Figure 3. N2LO LIT of the deuteron response for $\Lambda = 1600$ MeV, $\sigma_I = 3.0$ MeV for momentum transfer (a) $q^2 = 0.1$ fm $^{-2}$, (b) $q^2 = 0.5$ fm $^{-2}$ and (c) $q^2 = 1.0$ fm $^{-2}$.

C. Confronting experimental data

Having analyzed in detail the convergence and systematics of our LIT calculation, we can finally confront experimental data to assess our results. In particular, this comparison provides new insights into the performance of the perturbatively renormalized Chiral EFT interaction that we are using. In order to carry out this comparison, we need to invert the LIT and from it reconstruct the original response function. There is ample discussion in the literature that explains how delicate this inversion is in practice, as it falls into a category of technically ill-

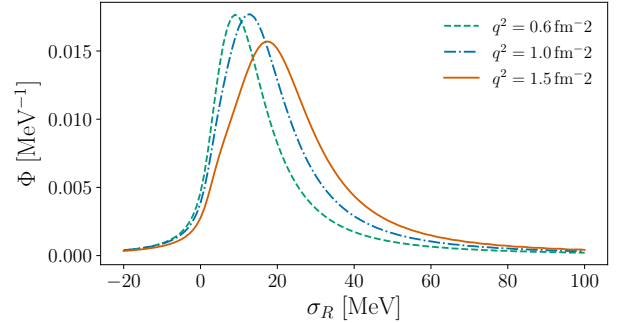


Figure 4. N2LO LIT of the deuteron response for $\Lambda = 800$ MeV, $\sigma_I = 3.0$ MeV for momentum transfer $q^2 = 0.6$ fm $^{-2}$, 1.0 fm $^{-2}$, 1.5 fm $^{-2}$.

posed problems [28]. The issue is that multiple different response functions can lead to all but identical Lorentz transforms, so that as a mapping of functions the LIT is almost not invertible – especially in the practical numerical calculations, where one always only ever has the functions defined on finite domains, and where one generally has to work with finite-precision floating-point numbers. A typical phenomenon is that the inversion can lead to high-frequency oscillations in the reconstructed response, which get averaged out if one completes the circle by applying again the LIT [28].

All that said, with sufficient care it *is* possible to perform successful LIT inversions. We employ here a variant of the expansion method introduced already in Ref. [27], the details of which are explained in Appendix C. In Fig. 5 we compare the response obtained from inverting the LIT, calculated for momentum transfer $q^2 = 0.6$ fm $^{-2}$ with EFT cutoff $\Lambda = 800$ MeV and $\sigma_I = 3.0$ MeV to experimental data of Simon *et al.* [49].⁵ For this comparison we note that different conventions for expressing the electro-disintegration cross section in terms of response functions exist in the literature. For the theory calculation, we followed Refs. [31–34], while Ref. [49] uses the convention of Fabian and Arenhövel [50].⁶ A careful comparison of conventions (see also Ref. [51]) along with reducing all kinematic quantities non-relativistically (consistent with our perturbative treatment of relativistic corrections) ultimately yields that we need to multiply our response function by a factor $2\pi^2\alpha$ in order to compare to the experimental data of Simon *et al.* [49].

Including this factor, we obtain the results shown in Figs. 5 and 6 for the longitudinal response function at $q^2 = 0.6$ fm $^{-2}$ and $q^2 = 1.0$ fm $^{-2}$, respectively. In these figures, we include two sources of uncertainty: the uncertainty due to the inversion procedure and the EFT

⁵ Specifically, this data has been taken from Table 1 in Ref. [49].

⁶ A comment in Ref. [50] furthermore suggests that the factor $\omega^{c.m.}$ in Eq. (1) of Ref. [49] is a typographical error, and consequently we dropped it in order to match conventions to ours.

uncertainty. As outlined in Appendix C, the inversion procedure generates a band with upper and lower bounds $R_{\max/\min}$. To include the EFT uncertainty in addition, we apply factors $1 \pm \lambda_n$ to the upper and lower bounds of the inversion bands, with $\lambda_n = (Q/M_{\text{hi}})^{n+1}$ and n the EFT order. For the breakdown scale, we again follow Ref. [22] and use the delta-nucleon mass splitting, $M_{\text{hi}} = \delta \simeq 300 \text{ MeV}$, as a conservative estimate. For deuteron disintegration, we follow Ref. [52] and identify the outgoing momentum of the np -pair,

$$|\mathbf{p}'| = \sqrt{(\omega - B)M_N + \mathbf{q}^2 \frac{M_N}{2M_d}} \quad (45)$$

as one relevant scale for the EFT analysis, in addition to the momentum transfer $|\mathbf{q}|$. For estimating the uncertainty, we set

$$Q = \max(|\mathbf{p}'|, |\mathbf{q}|) \quad (46)$$

to determine λ_n . Overall we find that our theoretical calculation of the response function agrees well with the experimental data, and that it exhibits good convergence with respect to the Chiral EFT expansion.

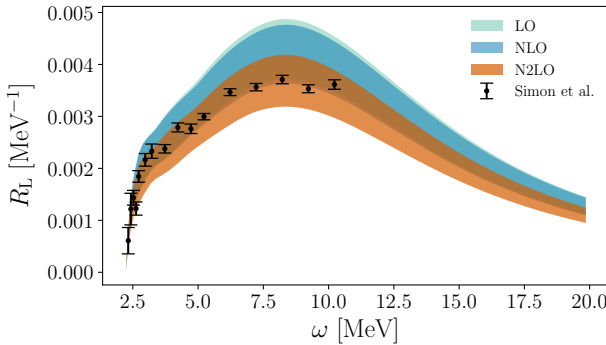


Figure 5. Deuteron response from the inverted LIT for $\Lambda = 800 \text{ MeV}$, $\sigma_I = 3.0 \text{ MeV}$ for momentum transfer $\mathbf{q}^2 \approx 0.6 \text{ fm}^{-2}$ for orders LO, NLO, N2LO. The experimental data presented are from Ref. [49].

IV. SUMMARY AND OUTLOOK

In this work, we have studied deuteron electrodisintegration in Chiral EFT, using the power counting of Refs. [22–25] to achieve a consistently renormalized formulation of the theory. To maintain this renormalization order by order, we follow a rigorously perturbative approach that treats only LO non-perturbatively and includes all higher-order corrections in distorted-wave perturbation theory. As we utilize the LIT method in order to calculate the longitudinal response function for the electrodisintegration process, a key result of our work is the derivation of the perturbative expansion for the LIT equations, which we formulate in momentum space,

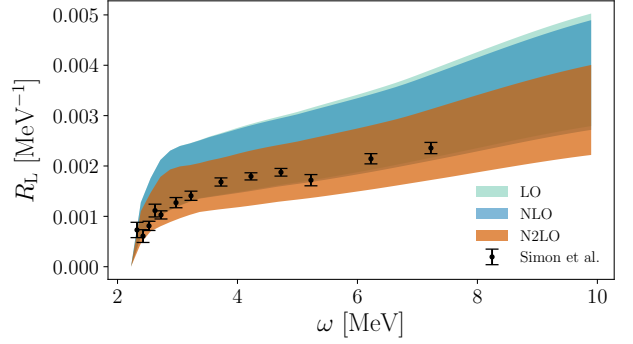


Figure 6. Deuteron response from the inverted LIT $\Lambda = 800 \text{ MeV}$, $\sigma_I = 3.0 \text{ MeV}$ for momentum transfer $\mathbf{q}^2 \approx 1.0 \text{ fm}^{-2}$ for orders LO, NLO, N2LO. The experimental data presented are from Ref. [49].

inspired by Ref. [34]. Our numerical calculations demonstrate that the methods work well, and, by studying variation of the EFT cutoff, we find that the theory is properly renormalized for the breakup observable that we study. To the best of our knowledge, this has not been previously tested within this framework. Moreover, we find that our EFT results are in good agreement with experimental data available within the range of energies that we would (Delta-less) Chiral EFT to be valid in. Our results therefore pave the way for future studies of inelastic processes in a range of nuclei, using perturbatively renormalized Chiral EFT, either in the “minimally modified Weinberg (MMW)” approach adopted in this work, and also using recently suggested novel schemes for Chiral EFT with fully perturbative pions [53, 54]. Concretely, we plan concrete investigations along these lines for light nuclei ($A \geq 3$), which can be treated within the momentum-space Faddeev/Faddeev-Yakubowsky framework of Refs. [54–56]. In particular, it would be interesting to study the monopole transition in ${}^4\text{He}$, which has received a lot of attention in recent years [51, 57–61], within our framework.

ACKNOWLEDGMENTS

We thank Hang Yu, Nuwan Yapa, Winfried Leidemann, Giuseppina Orlandini, Sonia Bacca, Francesca Bonaiti, Xincheng Lin, Atul Kedia, and Daniel Phillips for useful discussions. We furthermore thank Rui Peng for preparing the matrix elements of the chiral potentials used in this work. This work was supported in part by the U.S. National Science Foundation (Grant No. PHY-2044632) and by the National Natural Science Foundation of China (NSFC) under the Grants Nos. 12275185 and 12335002. This material is based upon work supported by the U.S. Department of Energy, Office of Science, Office of Nuclear Physics, under the FRIB Theory Alliance, Award No. DE-SC0013617. Computational

resources for parts of this work were provided by the high-performance computing cluster operated by North Carolina State University.

Appendix A: Perturbative expansion of the deuteron wave function

As mentioned in the main text, evaluating the LIT in a perturbative manner relies on a perturbative expansion of the deuteron bound state that appears on the right-hand side of Eq. (15b). To find this perturbative expansion, one can start from the Schrödinger equation written as

$$(E - H_0) |\psi\rangle = V |\psi\rangle. \quad (\text{A1})$$

Expanding both $E = E^{(0)} + E^{(1)} + E^{(2)} + \dots$ and $|\psi\rangle = |\psi^{(0)}\rangle + |\psi^{(1)}\rangle + |\psi^{(2)}\rangle + \dots$, along with V as described in Eq. (17) leads to equations of the form

$$(E^{(0)} - H_0) |\psi^{(0)}\rangle = V^{(0)} |\psi^{(0)}\rangle \quad (\text{A2a})$$

$$(E^{(0)} - H_0) |\psi^{(1)}\rangle = V^{(0)} |\psi^{(1)}\rangle + (V^{(1)} - E^{(1)}) |\psi^{(0)}\rangle \quad (\text{A2b})$$

$$(E^{(0)} - H_0) |\psi^{(2)}\rangle = V^{(0)} |\psi^{(2)}\rangle + (V^{(1)} - E^{(1)}) |\psi^{(1)}\rangle + (V^{(2)} - E^{(2)}) |\psi^{(0)}\rangle. \quad (\text{A2c})$$

Using the definition of the free Green's function,

$$G_0(z) = (z - H_0)^{-1}, \quad (\text{A3})$$

evaluated at the leading order binding energy $z = E^{(0)} = -B^{(0)}$, these equations can be rewritten as

$$(G_0 V^{(0)} - 1) |\psi^{(0)}\rangle = 0 \quad (\text{A4a})$$

$$(G_0 V^{(0)} - 1) |\psi^{(1)}\rangle = G_0 (E^{(1)} - V^{(1)}) |\psi^{(0)}\rangle \quad (\text{A4b})$$

$$(G_0 V^{(0)} - 1) |\psi^{(2)}\rangle = G_0 (E^{(1)} - V^{(1)}) |\psi^{(1)}\rangle + G_0 (E^{(2)} - V^{(2)}) |\psi^{(0)}\rangle. \quad (\text{A4c})$$

Alternatively, one can directly rewrite Eq. (A1) in terms of $G_0(E)$ and perturbatively expand the resulting expression.

Appendix B: Multipole and partial-wave expansion of the current operators

We wish to expand any generic operator $\rho(\mathbf{q})$ into multipoles, as stated in Eq. (7) in the main text. This expansion will arise naturally from expressing $\rho(\mathbf{q})$ in the momentum-space partial-wave basis, the details of which are provided in the following subsections.

1. Leading-order charge operator

For the LO charge density operator $\rho^{(0)}(\mathbf{q})$, we start by separating the spatial and discrete parts as

$$\rho^{(0)}(\mathbf{q}) = \tilde{\rho}^{(0)}(\mathbf{q}) \sum_{i=1,2} \frac{1 + \tau_3^{(i)}}{2}, \quad (\text{B1})$$

where $\tau_3^{(i)}$ is a Pauli matrix acting on nucleon i in isospin space, and

$$\langle \mathbf{p} | \tilde{\rho}^{(0)}(\mathbf{q}) | \mathbf{p}' \rangle = \delta^{(3)}(\mathbf{p} - \mathbf{p}' - \frac{1}{2}\mathbf{q}), \quad (\text{B2})$$

in momentum space, where the factor $1/2$ stems from embedding the one-body operator into a two-nucleon space expressed in relative coordinates.

We use u in the following to denote momenta and write two-nucleon partial-wave states as $|u; \alpha\rangle = |u; (ls)j, t\rangle$. To further evaluate the charge density operator, we need to decouple the spatial part according to

$$|u; (ls)j, t\rangle = \sum_{m, m_s} C_{lm, sm_s}^{j\cdot} |u; lm\rangle |sm_s; t\rangle. \quad (\text{B3})$$

Note that we are omitting here the projection quantum number associated with the total angular momentum j , indicated with the ‘ \cdot ’ on the Clebsch-Gordan coefficient.

Focusing first on the spatial part of the operator, we have to evaluate

$$\begin{aligned} & \langle u; lm | \tilde{\rho}^{(0)}(\mathbf{q}) | u'; l'm' \rangle \\ &= \int d^3p \int d^3p' \langle u; lm | \mathbf{p} \rangle \langle \mathbf{p} | \tilde{\rho}^{(0)}(\mathbf{q}) | \mathbf{p}' \rangle \langle \mathbf{p}' | u'; l'm' \rangle \\ &= \int d^3p \int d^3p' Y_{lm}(\hat{\mathbf{p}}) \frac{\delta(u - p)}{u^2} \delta^{(3)}(\mathbf{p} - \mathbf{p}' - \frac{1}{2}\mathbf{q}) \\ & \quad \times Y_{l'm'}^*(\hat{\mathbf{p}}') \frac{\delta(u' - p')}{u'^2} \\ &= \int dp p^2 \int d\Omega_p Y_{lm}(\hat{\mathbf{p}}) \frac{\delta(u - p)}{u^2} \frac{\delta(u' - |\mathbf{p} - \frac{1}{2}\mathbf{q}|)}{u'^2} \\ & \quad \times Y_{l'm'}^*(\widehat{\mathbf{p} - \frac{1}{2}\mathbf{q}}). \end{aligned} \quad (\text{B4})$$

Above the names of vectors, we use the hat symbol to denote the angular part in a spherical representation of the vector.

We proceed to modify this expression, using techniques described in Ref. [62] for the permutation operators appearing in the Faddeev equations, and expanding upon a similar discussion in Ref. [55] (which we reproduce here to keep this section self-contained) to keep track of all multipoles. To begin, we note that

$$\begin{aligned} \frac{\delta(u' - |\mathbf{p} - \frac{1}{2}\mathbf{q}|)}{u'^2} &= 2\pi \sum_k \sqrt{\hat{k}} (-1)^k \left[\int_{-1}^1 dx P_k(x) \right. \\ & \quad \times \left. \frac{\delta(u' - \sqrt{p^2 - p q x + q^2/4})}{u'^2} \right] \mathcal{Y}_{kk}^{00}(\hat{\mathbf{p}}, \hat{\mathbf{q}}), \end{aligned} \quad (\text{B5})$$

where $\mathcal{Y}_{l_1, l_2}^{LM}$ is used to denote two coupled spherical harmonics. Moreover,

$$Y_{l'm'}^*(\widehat{\mathbf{p} - \frac{1}{2}\mathbf{q}}) = \sum_{\lambda'_1 + \lambda'_2 = l'} \frac{p^{\lambda'_1} \left(-\frac{1}{2}q\right)^{\lambda'_2}}{|\mathbf{p} - \frac{1}{2}\mathbf{q}|^{l'}} \times \sqrt{\frac{4\pi(2l'+1)!}{(2\lambda'_1+1)!(2\lambda'_2+1)!}} \mathcal{Y}_{\lambda'_1 \lambda'_2}^{l'm'*}(\hat{\mathbf{p}}, \hat{\mathbf{q}}). \quad (\text{B6})$$

Inserting these into Eq. (B4) gives

$$\begin{aligned} \langle u; lm | \tilde{\rho}^{(0)}(\mathbf{q}) | u'; l'm' \rangle &= \int dp p^2 d\hat{\mathbf{p}} Y_{lm}(\hat{\mathbf{p}}) \frac{\delta(u-p)}{u^2} \\ &\times 2\pi \sum_k \sqrt{\hat{k}} (-1)^k \left[\int_{-1}^1 dx P_k(x) \frac{\delta(u' - \sqrt{p^2 - pqx + q^2/4})}{u'^2} \right] \mathcal{Y}_{kk}^{00}(\hat{\mathbf{p}}, \hat{\mathbf{q}}) \\ &\times \sum_{\lambda'_1 + \lambda'_2 = l'} \frac{p^{\lambda'_1} \left(-\frac{1}{2}q\right)^{\lambda'_2}}{|\mathbf{p} - \frac{1}{2}\mathbf{q}|^{l'}} \sqrt{\frac{4\pi(2l'+1)!}{(2\lambda'_1+1)!(2\lambda'_2+1)!}} \mathcal{Y}_{\lambda'_1 \lambda'_2}^{l'm'*}(\hat{\mathbf{p}}, \hat{\mathbf{q}}). \quad (\text{B7}) \end{aligned}$$

The product of two coupled spherical harmonics can be reduced as follows:

$$\begin{aligned} \mathcal{Y}_{\lambda'_1 \lambda'_2}^{l'm'*}(\hat{\mathbf{p}}, \hat{\mathbf{q}}) \mathcal{Y}_{kk}^{00}(\hat{\mathbf{p}}, \hat{\mathbf{q}}) &= \frac{1}{4\pi} \sqrt{\hat{k} \lambda'_1 \lambda'_2} (-1)^{\lambda'_1 + \lambda'_2 + l'} \\ &\times \sum_{f_1, f_2} \left\{ \begin{matrix} f_2 & f_1 & l' \\ \lambda'_1 & \lambda'_2 & k \end{matrix} \right\} C_{k0, \lambda'_1 0}^{f_1 0} C_{k0, \lambda'_2 0}^{f_2 0} \mathcal{Y}_{f_1 f_2}^{l'm'*}(\hat{\mathbf{p}}, \hat{\mathbf{q}}). \quad (\text{B8}) \end{aligned}$$

We can now perform the integral over $\hat{\mathbf{p}}$ in Eq. (B7):

$$\int d\Omega_p Y_{lm}(\hat{\mathbf{p}}) \mathcal{Y}_{f_1 f_2}^{l'm'*}(\hat{\mathbf{p}}, \hat{\mathbf{q}}) = \sum_{m_2} C_{lm, f_2 m_2}^{l'm'} Y_{f_2 m_2}^*(\hat{\mathbf{q}}) \delta_{f_1 l}. \quad (\text{B9})$$

Noting that choosing \mathbf{q} aligned with the \hat{z} axis collapses the sum to just $m_2 = 0$ and then renaming $f_2 \rightarrow L$ establishes the connection with Eq. (7), and we have

$$Y_{L0}^*(q\hat{z}) = \frac{\sqrt{\hat{L}}}{\sqrt{4\pi}}. \quad (\text{B10})$$

Overall, collecting the various terms, we arrive at

$$\begin{aligned} \langle u; lm | \tilde{\rho}^{(0)}(\mathbf{q}) | u'; l'm' \rangle &= \int dp p^2 \frac{\delta(u-p)}{u^2} \sum_L \sqrt{\hat{L}} C_{lm, L0}^{l'm'} \times \frac{1}{2} \sum_k \sqrt{\hat{k}} (-1)^k \\ &\int_{-1}^1 dx P_k(x) \frac{\delta(u' - \sqrt{p^2 - pqx + q^2/4})}{u'^2} \sum_{\lambda'_1 + \lambda'_2 = l'} \frac{p^{\lambda'_1} \left(-\frac{1}{2}q\right)^{\lambda'_2}}{|\mathbf{p} - \frac{1}{2}\mathbf{q}|^{l'}} \sqrt{\frac{(2l'+1)!}{(2\lambda'_1+1)!(2\lambda'_2+1)!}} \sqrt{\hat{k} \lambda'_1 \lambda'_2} (-1)^{\lambda'_1 + \lambda'_2 + l'} \\ &\times \left\{ \begin{matrix} L & l & l' \\ \lambda'_1 & \lambda'_2 & k \end{matrix} \right\} C_{k0, \lambda'_1 0}^{l 0} C_{k0, \lambda'_2 0}^{L 0}, \quad (\text{B11}) \end{aligned}$$

which can be grouped as

$$\langle u; lm | \tilde{\rho}^{(0)}(\mathbf{q}) | u'; l'm' \rangle = \sum_L \sqrt{\hat{L}} \langle u; lm | \tilde{\rho}_L^{(0)}(q) | u'; l'm' \rangle = \sum_L \sqrt{\hat{L}} C_{lm, L0}^{l'm'} \langle u; l | \tilde{\rho}_L^{(0)}(q) | u'; l' \rangle. \quad (\text{B12})$$

This is exactly the form that is to be expected from the

Wigner-Eckart theorem, and we note that the Clebsch-

Gordan coefficient $C_{lm,L0}^{l'm'}$ implies $m = m'$, which is a consequence of our choice of \mathbf{q} aligned with the z axis. Eliminating also the integral over p , the final result for the reduced matrix element can be written as

$$\langle u; l | \tilde{\rho}_L^{(0)}(q) | u'; l' \rangle = \int_{-1}^1 dx G_{l,l'}^L(u, q, x) \frac{\delta(u' - \iota(u, q, x))}{u'^2} \quad (\text{B13})$$

with

$$G_{l,l'}^L(u, q, x) = \frac{1}{2} \sum_k \sqrt{\hat{k}} (-1)^k P_k(x) \sum_{\lambda'_1 + \lambda'_2 = l'} \frac{u^{\lambda'_1} \left(-\frac{1}{2}q\right)^{\lambda'_2}}{\iota(u, q, x)^{l'}} \sqrt{\frac{(2l'+1)!}{(2\lambda'_1+1)!(2\lambda'_2+1)!}} \sqrt{\hat{k} \lambda'_1 \lambda'_2} (-1)^{\lambda'_1 + \lambda'_2 + l'} \times \begin{Bmatrix} L & l & l' \\ \lambda'_1 & \lambda'_2 & k \end{Bmatrix} C_{k0, \lambda'_1 0}^{l0} C_{k0, \lambda'_2 0}^{l0}. \quad (\text{B14})$$

Since the charge density operator does not couple to the nucleon spins, including that amounts to a simple recoupling symbol,

$$\begin{aligned} \langle u; (ls)jm_j | \tilde{\rho}_L(\mathbf{q}) | u'; (l's')j'm'_j \rangle &= (-1)^{j+s+l'+L} \sqrt{\hat{j}\hat{l}} C_{jm_j, L0}^{j'm'_j} \begin{Bmatrix} l & s & j \\ j' & L & l' \end{Bmatrix} \delta_{ss'} \langle u; l | \tilde{\rho}_{L0}(\mathbf{q}) | u'; l' \rangle \\ &\equiv C_{jm_j, L0}^{j'm'_j} \langle u; (ls)j | \tilde{\rho}_L(q) | u'; (l's')j' \rangle, \end{aligned} \quad (\text{B15})$$

and overall we have defined, in the second line, the reduced matrix element in the spin-orbit coupled basis.

Finally, the isospin part can be evaluated by writing a two-nucleon coupled isospin state as

$$|tm_t\rangle = \sum_{m_1, m_2} C_{t_1 m_1, t_2 m_2}^{tm_t} |t_1 m_1\rangle |t_2 m_2\rangle \quad (\text{B16})$$

so that

$$\begin{aligned} \langle tm_t | \frac{1 + \tau_3^{(i)}}{2} | t'm'_t \rangle \\ = \sum_{m_1, m_2} C_{t_1 m_1, t_2 m_2}^{tm_t} C_{t_1 m_1, t_2 m_2}^{t'm'_t} \frac{1 + m_i}{2}. \end{aligned} \quad (\text{B17})$$

derive the partial wave representation of this operator, we begin by recoupling the spin and spatial parts in spherical tensor form

$$\begin{aligned} 2i\mathbf{q} \cdot \boldsymbol{\sigma}_1 \times \mathbf{K} &= i\mathbf{q} \cdot \boldsymbol{\sigma}_1 \times (\mathbf{p} + \mathbf{p}' - \mathbf{q}/2) \\ &= \sqrt{6} \{ \sigma_1^1 \otimes [q^1 \otimes (\mathbf{p} + \mathbf{p}' - \mathbf{q}/2)^1]^1 \}^{00}. \end{aligned} \quad (\text{B18})$$

2. Next-to-next-to-leading order charge operator

At N2LO, there is a relativistic correction to the LO charge operator, shown in Eq. (35a) in the main text. To

With Eq. (B3), we can decouple the spin and spatial parts as

$$\begin{aligned} \langle u; (ls)jm_j | \{ \sigma_i^1 \otimes [q^1 \otimes (\mathbf{p} + \mathbf{p}' - \mathbf{q}/2)^1]^1 \}^{00} | u'; (l's')j'm'_j \rangle \\ = \sum_{\nu\mu} \sum_{mm'} \sum_{m_s m'_s} C_{1\nu, 1\mu}^{00} C_{lm, sm_s}^{jm_j} C_{l'm', s'm'_s}^{j'm'_j} \langle sm_s | \sigma_i^{1\nu} | s'm'_s \rangle \times \langle u; lm | [q^1 \otimes (\mathbf{p} + \mathbf{p}' - \mathbf{q}/2)^1]^{1\mu} | u'; lm' \rangle \end{aligned} \quad (\text{B19})$$

Considering the spatial part, we need to calculate

$$\begin{aligned}
\langle u; lm | [q^1 \otimes (\mathbf{p} + \mathbf{p}' - \mathbf{q}/2)^1]^1 \mu \delta^{(3)}(\mathbf{p} - \mathbf{p}' - \frac{1}{2}\mathbf{q}) | u'; l' m' \rangle \\
= \int d^3p \int d^3p' Y_{lm}^*(\hat{\mathbf{p}}) \frac{\delta(u-p)}{u^2} [q^1 \otimes (\mathbf{p} + \mathbf{p}' - \mathbf{q}/2)^1]^1 \mu \delta^{(3)}(\mathbf{p} - \mathbf{p}' - \mathbf{q}/2) Y_{l'm'}(\hat{\mathbf{p}}') \frac{\delta(u'-p')}{u'^2} \\
= \int d^3p \int d^3p' Y_{lm}^*(\hat{\mathbf{p}}) \frac{\delta(u-p)}{u^2} \delta^{(3)}(\mathbf{p} - \mathbf{p}' - \mathbf{q}/2) Y_{l'm'}(\hat{\mathbf{p}}') \frac{\delta(u'-p')}{u'^2} \\
\times \frac{4\pi}{3} |\mathbf{q}| |\mathbf{p} + \mathbf{p}' - \mathbf{q}/2| \sum_{\lambda_1, \lambda_2=-1}^1 C_{1\lambda_1, 1\lambda_2}^{1\mu} Y_{1\lambda_1}(\hat{\mathbf{q}}) Y_{1\lambda_2}(\mathbf{p} + \mathbf{p}' - \frac{1}{2}\mathbf{q}). \quad (B20)
\end{aligned}$$

We follow the same procedure as in Sec. B 1, *i.e.*, we integrate over \mathbf{p}' and expand $x \equiv \hat{\mathbf{q}} \cdot \hat{\mathbf{p}}$ in terms of Legendre polynomials. We also need the contraction rule for spherical harmonics:

$$\begin{aligned}
& Y_{l'm'}(\widehat{\mathbf{p} - \frac{1}{2}\mathbf{q}}) Y_{1\lambda_2}(\widehat{\mathbf{p} - \frac{1}{2}\mathbf{q}}) \\
= & \sum_{\beta\beta_m} \sqrt{\frac{3\hat{\beta}}{4\pi\hat{\beta}}} C_{l'0,10}^{\beta 0} C_{l'm',1\lambda_2}^{\beta\beta_m} Y_{\beta\beta_m}(\widehat{\mathbf{p} - \frac{1}{2}\mathbf{q}}). \quad (B21)
\end{aligned}$$

After reducing the product of two coupled spherical har-

monics as in Eq. (B8),

$$\begin{aligned}
Y_{\gamma_1\gamma_2}^{\beta\beta_m}(\hat{\mathbf{p}}, \hat{\mathbf{q}}) Y_{kk}^{00}(\hat{\mathbf{p}}, \hat{\mathbf{q}}) &= \frac{1}{4\pi} \sqrt{\hat{k}\hat{\gamma}_1\hat{\gamma}_2} (-1)^{\beta+\gamma_1+\gamma_2} \\
\times \sum_{f_1, f_2} \left\{ \begin{matrix} f_2 & f_1 & \beta \\ \gamma_1 & \gamma_2 & k \end{matrix} \right\} C_{k0, \gamma_1 0}^{f_1 0} C_{k0, \gamma_2 0}^{f_2 0} Y_{f_1 f_2}^{\beta\beta_m}(\hat{\mathbf{p}}, \hat{\mathbf{q}}), \quad (B22)
\end{aligned}$$

the integral over $\hat{\mathbf{p}}$ can be completed as in Eq. (B9):

$$\begin{aligned}
& \int d\Omega_p Y_{lm}^*(\hat{\mathbf{p}}) Y_{f_1 f_2}^{\beta\beta_m}(\hat{\mathbf{p}}, \hat{\mathbf{q}}) \\
= & \sum_{m_1 m_2} C_{f_1 m_1, f_2 m_2}^{\beta\beta_m} Y_{f_2 m_2}(\hat{\mathbf{q}}) \delta_{f_1 l} \delta_{mm_1}. \quad (B23)
\end{aligned}$$

By collecting these terms together and integrating out p , we arrive at the following:

$$\begin{aligned}
& \langle u; lm | [q^1 \otimes (\mathbf{p} + \mathbf{p}' - \mathbf{q}/2)^1]^1 \mu \delta^{(3)}(\mathbf{p} - \mathbf{p}' - \frac{1}{2}\mathbf{q}) | u'; l' m' \rangle \\
= & \frac{4\pi}{\sqrt{3}} q \sum_k \hat{k} (-1)^k \int_{-1}^1 dx P_k(x) \frac{\delta(u' - \iota(u, q, x))}{u'^2} \sum_{\lambda_1, \lambda_2=-1}^1 C_{1\lambda_1, 1\lambda_2}^{1\mu} \sum_{\beta\beta_m} \sqrt{\hat{\beta}} C_{l'0,10}^{\beta 0} C_{l'm',1\lambda_2}^{\beta\beta_m} \sum_{\gamma_1+\gamma_2=\beta} \frac{u^{\gamma_1} (-\frac{q}{2})^{\gamma_2}}{(\iota(u, q, x))^{\beta-1}} \\
\times & \sqrt{\binom{2\beta}{2\gamma_1}} \times \sum_{f_2} \left\{ \begin{matrix} f_2 & l & \beta \\ \gamma_1 & \gamma_2 & k \end{matrix} \right\} C_{k0, \gamma_1 0}^{f_1 0} C_{k0, \gamma_2 0}^{f_2 0} \sum_{m_2} C_{l'm', f_2 m_2}^{\beta\beta_m} Y_{f_2 m_2}(\hat{\mathbf{q}}) Y_{1\lambda_1}(\hat{\mathbf{q}}), \quad (B24)
\end{aligned}$$

where

$$\iota(p, q, x) = \sqrt{p^2 - pqx + q^2/4}. \quad (B25)$$

Contracting two spherical harmonics depending on $\hat{\mathbf{q}}$, we get

$$\begin{aligned}
& Y_{f_2 m_2}(\hat{\mathbf{q}}) Y_{1\lambda_1}(\hat{\mathbf{q}}) \\
= & \sum_{L m_L} \sqrt{\frac{3\hat{f}_2}{4\pi\hat{L}}} C_{f_2 0, 10}^{L 0} C_{f_2 m_2, 1\lambda_1}^{L m_L} Y_{L m_L}(\hat{\mathbf{q}}). \quad (B26)
\end{aligned}$$

Here L is the rank of multipole, as in Sec. B 1. Choosing

\mathbf{q} aligned with the \hat{z} axis leads to $m_L = 0$ and Eq. (B10). The sums over $\lambda_1, \lambda_2, \beta_m$ and m_2 can be carried out explicitly by employing relations for sums of products of Clebsch-Gordan coefficients [63]:

$$\begin{aligned}
& \sum_{\substack{\lambda_1, \lambda_2 \\ \beta_m m_2}} C_{1\lambda_1, 1\lambda_2}^{1\mu} C_{l'm', 1\lambda_2}^{\beta\beta_m} C_{l'm', f_2 m_2}^{\beta\beta_m} C_{f_2 m_2, 1\lambda_1}^{L 0} \\
= & (-1)^{l+l'+f_2-2\beta} \times (-1)^{L-1+m-m'} \\
\times & \hat{\beta} \sqrt{1\hat{L}} \sum_{k\kappa} C_{l'm', L 0}^{k\kappa} C_{l'm', 1-\mu}^{k\kappa} \left\{ \begin{matrix} 1 & 1 & 1 \\ f_2 & \beta & l \\ L & l' & k \end{matrix} \right\}. \quad (B27)
\end{aligned}$$

Finally, the spatial part can be simplified as

$$\begin{aligned}
& \langle u l m | [q^1 \otimes (\mathbf{p} + \mathbf{p}' - \mathbf{q}/2)^1]^1 \mu \delta^{(3)}(\mathbf{p} - \mathbf{p}' - \frac{1}{2}\mathbf{q}) | u' l' m' \rangle \\
&= q \sqrt{\hat{l}'} \sum_L \sqrt{\hat{L}} \sum_k \hat{k} (-1)^k \int_{-1}^1 dx P_k(x) \frac{\delta(u' - \iota(u, q, x))}{u'^2} \sum_{\beta} C_{l'0,10}^{\beta 0} \sum_{\gamma_1 + \gamma_2 = \beta} \sqrt{\binom{2\beta}{2\gamma_1}} \frac{p^{\gamma_1} (-\frac{q}{2})^{\gamma_2}}{(\iota(u, q, x))^{\beta-1}} \\
&\quad \times \sum_{f_2} \sqrt{\frac{\hat{f}_2}{\hat{L}}} \begin{Bmatrix} f_2 & l & \beta \\ \gamma_1 & \gamma_2 & k \end{Bmatrix} \times C_{k0,\gamma_1 0}^{l0} C_{k0,\gamma_2 0}^{f_2 0} C_{f_2 0,10}^{L0} \times (-1)^{l+l'+f_2-2\beta} \times (-1)^{L-1+m-m'} \\
&\quad \times \hat{\beta} \sqrt{\hat{1}\hat{L}} \sum_{\bar{k}\kappa} C_{l'm',L0}^{\bar{k}\kappa} C_{lm,1-\mu}^{\bar{k}\kappa} \begin{Bmatrix} 1 & 1 & 1 \\ f_2 & \beta & l \\ L & l' & \bar{k} \end{Bmatrix}, \quad (\text{B28})
\end{aligned}$$

and the spin part can be evaluated in the same way as the isospin part:

$$\langle s m_s | \sigma_i^{1\nu} | s' m'_s \rangle = (-1)^{s'} \sqrt{6\hat{s}'} C_{s'm'_s,1\nu}^{sm_s} \begin{Bmatrix} \frac{1}{2} & s & \frac{1}{2} \\ s' & \frac{1}{2} & 1 \end{Bmatrix}. \quad (\text{B29})$$

Inserting Eqs. (B28) and (B29) into Eq. (B19), and evaluating following sums explicitly:

$$\begin{aligned}
& \sum_{\nu\mu} \sum_{m_l m'_l} \sum_{m_s m'_s} \sum_{\kappa} (-1)^{m_l - m'_l} C_{1\nu,1\mu}^{00} C_{lm_l,sm_s}^{jm_j} C_{l'm'_l,s'm'_s}^{j'm'_j} C_{l'm'_l,L0}^{\bar{k}\kappa} C_{lm_l,1-\mu}^{\bar{k}\kappa} C_{s'm'_s,1\nu}^{sm_s} \\
&= (-1)^{l+L+\bar{k}+s'-s+1} \sqrt{\frac{\hat{j}\hat{s}}{3}} C_{jm_j,L0}^{j'm'_j} \hat{k} \begin{Bmatrix} l' & s' & j' \\ j & L & \bar{k} \end{Bmatrix} \begin{Bmatrix} l & s & j \\ s' & \bar{k} & 1 \end{Bmatrix}, \quad (\text{B30})
\end{aligned}$$

we arrive at the final result

$$\begin{aligned}
& \langle u; (ls) j m_j | 2i\mathbf{q} \cdot \boldsymbol{\sigma}_i \times \mathbf{K}_i \delta^{(3)}(\mathbf{p} - \mathbf{p}' - \frac{1}{2}\mathbf{q}) | u'; (l's') j' m'_j \rangle \\
&= 6\sqrt{\hat{s}\hat{s}'} \times (-1)^{l'-s} \sqrt{\hat{j}\hat{l}'} \begin{Bmatrix} \frac{1}{2} & s & \frac{1}{2} \\ s' & \frac{1}{2} & 1 \end{Bmatrix} \times q \sum_L \sqrt{\hat{L}} C_{jm_j,L0}^{j'm'_j} \sum_k \hat{k} (-1)^k \int_{-1}^1 dx P_k(x) \frac{\delta(u' - \iota(u, q, x))}{u'^2} \\
&\quad \times \sum_{\beta} \hat{\beta} \sum_{\gamma_1 + \gamma_2 = \beta} \sqrt{\binom{2\beta}{2\gamma_1}} \frac{p^{\gamma_1} (-\frac{q}{2})^{\gamma_2}}{(\iota(u, q, x))^{\beta-1}} \sum_{f_2} (-1)^{f_2} \sqrt{\hat{f}_2} \begin{Bmatrix} f_2 & l & \beta \\ \gamma_1 & \gamma_2 & k \end{Bmatrix} C_{l'0,10}^{\beta 0} C_{k0,\gamma_1 0}^{l0} C_{k0,\gamma_2 0}^{f_2 0} C_{f_2 0,10}^{L0} \\
&\quad \times \sum_{\bar{k}} (-1)^{\bar{k}} \hat{k} \begin{Bmatrix} l' & s' & j' \\ j & L & \bar{k} \end{Bmatrix} \begin{Bmatrix} l & s & j \\ s' & \bar{k} & 1 \end{Bmatrix} \begin{Bmatrix} 1 & 1 & 1 \\ f_2 & \beta & l \\ L & l' & \bar{k} \end{Bmatrix}. \quad (\text{B31})
\end{aligned}$$

The isospin part can be evaluated easily as in Eq. (B17).

3. Effective boost-correction charge operator

As mentioned in Sec. II F 3, the corrections that arise from boosting the initial deuteron state from the lab frame into the final-state center-of-mass frame, which en-

ter at N2LO, can be written in terms of effective corrections to the current operator. To derive these, we start from Eq. (39) and consider the substitution $q \rightarrow q/\sqrt{1+\eta}$. Expanding the result up to first order in $\eta = q^2/(4M_d^2)$ leads to the following matrix element:

$$\begin{aligned}
& \langle u; lm | \rho_{\text{boost}}^{(2)}(\mathbf{q}) | u'; l'm' \rangle = \sum_L \sqrt{\hat{L}} C_{lm,L0}^{l'm'} \int_{-1}^1 dx \eta \times \left[G_{l,l'}^{L,\text{boost,a}}(u, q, x) \frac{\delta'(u' - \iota(u, q, x))}{u'^2} \right. \\
&\quad \left. + G_{l,l'}^{L,\text{boost,b}}(u, q, x) \frac{\delta(u' - \iota(u, q, x))}{u'^2} \right], \quad (\text{B32})
\end{aligned}$$

where

$$G_{l,l'}^{L,\text{boost,a}}(u, q, x) = \frac{G_{l,l'}^L(u, q, x)}{\iota(u, q, x)^2} \left(\frac{q^2}{8} - \frac{uqx}{4} \right), \quad (\text{B33a})$$

$$G_{l,l'}^{L,\text{boost,b}}(u, q, x) = \frac{l' G_{l,l'}^L(u, q, x)}{\iota(u, q, x)} \left(\frac{q^2}{8} - \frac{uqx}{4} \right) - \frac{\tilde{G}_{l,l'}^{L,\text{boost,b}}(u, q, x)}{\iota(u, q, x)}, \quad (\text{B33b})$$

and

$$\begin{aligned} \tilde{G}_{l,l'}^{L,\text{boost,b}}(u, q, x) = & \frac{1}{2} \sum_k \sqrt{\hat{k}} (-1)^k P_k(x) \sum_{\lambda'_1 + \lambda'_2 = l'} \frac{u^{\lambda'_1} \left(-\frac{1}{2}q\right)^{\lambda'_2}}{\iota(u, q, x)^{l'}} \frac{\lambda'_2}{2} \sqrt{\frac{(2l'+1)!}{(2\lambda'_1+1)!(2\lambda'_2+1)!}} \sqrt{\hat{k} \lambda'_1 \lambda'_2} (-1)^{\lambda'_1 + \lambda'_2 + l'} \\ & \times \begin{Bmatrix} L & l & l' \\ \lambda'_1 & \lambda'_2 & k \end{Bmatrix} C_{k0,\lambda'_1 0}^{l0} C_{k0,\lambda'_2 0}^{l0}. \end{aligned} \quad (\text{B34})$$

Appendix C: Inversion of the LIT

To invert the LIT, we follow the basic procedure discussed in Ref. [28], with certain extensions that we describe in this section. The basic idea of the approach is to expand the response function over a set of functions $\chi_n(\omega)$,

$$\mathcal{R}(\omega) = \sum_n \alpha_n \chi_n(\omega), \quad (\text{C1})$$

where α_n are coefficients to be determined. The precise form chosen for the $\chi_n(\omega)$ will be given below. Since the LIT as a mapping between functions is a linear operation, combining Eq. (C1) with Eq. (4) gives a related expansion for the LIT of the response function,

$$\Phi(\sigma_R) = \sum_n \alpha_n \tilde{\chi}_n(\sigma_R), \quad (\text{C2})$$

where the $\tilde{\chi}_n$ are given by

$$\tilde{\chi}_n(\sigma_R) = \int_{\omega_{\text{th}}}^{\infty} d\omega \frac{\chi_n(\omega)}{(\omega - \sigma_R)^2 + \sigma_I^2}. \quad (\text{C3})$$

That is, $\tilde{\chi}_n(\sigma_R)$ is just the LIT of $\chi_n(\omega)$, and the inversion is carried out by fitting Eq. (C2) to the LIT obtained as described in the main text. This procedure, while straightforward in principle, is still delicate in practice to the ill-posedness of the LIT inversion problem (see Sec. III C).

For the $\chi_n(\omega)$ it is important to choose a form that (a) is able to capture the actual structure of the response function and (b) ensures that the fit does not suffer from strong correlations among different $\chi_n(\omega)$. We further follow Ref. [28] in this regard and set

$$\chi_n(\omega) = e^{\beta_0} e^{-\epsilon \beta_1 / n}, \quad (\text{C4})$$

with $\epsilon = \omega - \omega_{\text{th}}$, and with β_0 and β_1 to be treated as nonlinear fit parameters. While Ref. [28] suggests to fix

β_0 based on physics considerations (enforcing a particular energy dependence at threshold), we find it more useful to let both β_0 and β_1 vary along with the linear fit parameters α_n . Moreover, also the optimal number N of terms in Eqs. (C1) and (C2) has to be determined empirically as part of the fitting procedure – too few terms will in general give a poor fit, but too many terms may lead to high-frequency oscillations and therefore unstable fits.

Instead of treating β_0 and β_1 on equal footing with the α_n in a combined non-linear fit, we chose to sample the two non-linear parameters across a relatively wide range, and then we run a linear fit for each sample of (β_0, β_1) to determine the corresponding α_n . For the linear fits, we perform Ridge regression (a regularized form of least squares) and ultimately calculate the linear coefficients using singular value decomposition (see, *e.g.* in Ref. [64], Chapter 4). This leads to an overall large collection of possible inversion results, many of which can be ruled out for poor performance (indicated by large fit residuals). Among the inversion candidates not ruled out in this way, there can still be some that feature implausible high-frequency oscillations. As discussed, this is, in general, a manifestation of the ill-posedness of the LIT inversion. We therefore choose to further filter the results by their behavior in Fourier space – implemented as a fast Fourier transform (FFT) – using the presence of significant power in the spectrum above a threshold frequency defined by the inverse width of the Lorentz kernel, $\xi_{\text{th}} = 1/2\pi\sigma_I$, as a natural criterion to discount a candidate inversion. This particular weight we use is the integral of the Fourier transform of the candidate response from ξ_{th} to infinity. As we are using the FFT, this is implemented in practice as a discrete sum of Fourier components between ξ_{th} and the maximum frequency determined by the discrete mesh used for ω (which, in turn, is determined by the σ_R mesh that the LIT was calculated on).

In practice we do not use a strict acceptance/rejection but rather sort all candidates by their performance – with respect to both fit residuals and high-frequency power.

Specifically, we found the following prescription to work well:

1. Out of the initial set of candidates from sampling and fitting, we keep the best N_{initial} out of N_{total} fits.
2. Those candidates we then sort by their Fourier weight, as defined above, and keep the best N_{Fourier} responses.
3. Out of these, we pick again the best N_{final} to calculate our final result for the response as the mean among those remaining candidates, with an uncertainty band provided by calculating the 97.5% percentile around the mean.

Reasonable values for N_{initial} , N_{Fourier} , and N_{final} , in addition to the number N of terms in Eq. (C1), still need to be determined empirically, but overall the inversion proceeds in an automatic fashion, and in practice one needs only ensure that all these numbers are large enough for the final result to become effectively independent of the particular choice.

As mentioned in the main text, a direct calculation of the deuteron response function is in fact a tractable task, which we have implemented at leading order in the EFT expansion. We can therefore use exact LO results to benchmark our inversion method. In Figs. 7, 8 we show results obtained from inverting LO LIT calculations at $\sigma_I = 3.0, 5.0, 10.0$ MeV compared to a direct calculation of the LO response function.

The values used to obtain the results presented in Fig. 7, 8 are $N = 15$, $N_{\text{initial}} = 200$, $N_{\text{Fourier}} = 20$ and $N_{\text{Final}} = 15, 10, 5$ as indicated in the legend. If one chooses smaller values for N_{initial} , there is a tendency to eliminate many of the smoother functions and one is left with only highly oscillatory results that are deemed unphysical for reasons discussed above. If one sorts by Fourier weight first, then the top-ranked results have relatively large residuals. The procedure remains independent of knowledge of the exact response function, which is important for cases where direct verification of inversion is unfeasible.

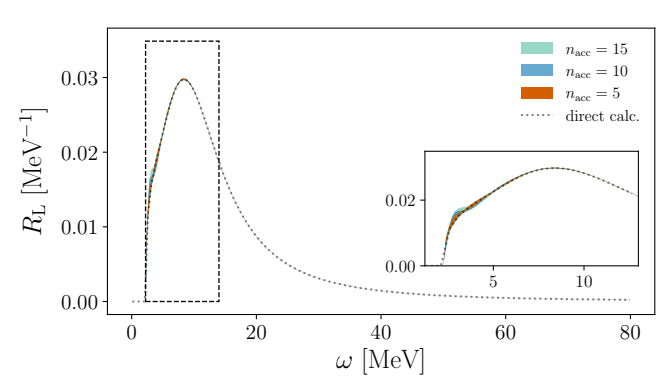


Figure 7. Deuteron response from the inverted LIT for $\Lambda = 800$ MeV, $\sigma_I = 3.0$ MeV for momentum transfer $\mathbf{q}^2 = 0.6$ fm^{-2} .

[1] H.-W. Hammer, S. König, and U. van Kolck, Rev. Mod. Phys. **92**, 025004 (2020).

[2] S. Weinberg, Phys. Lett. B **251**, 288 (1990).

[3] S. Weinberg, Nucl. Phys. B **363**, 3 (1991).

[4] C. Ordóñez and U. van Kolck, Phys. Lett. B **291**, 459 (1992).

[5] S. Weinberg, Phys. Lett. B **295**, 114 (1992), arXiv:hep-ph/9209257.

[6] U. L. Van Kolck, *Soft Physics: Applications of Effective Chiral Lagrangians to Nuclear Physics and Quark Models*, Ph.D. thesis, Texas U. (1993).

[7] M. Rho, Phys. Rev. Lett. **66**, 1275 (1991).

[8] T.-S. Park, D.-P. Min, and M. Rho, Phys. Rept. **233**, 341 (1993), arXiv:hep-ph/9301295.

[9] T.-S. Park, D.-P. Min, and M. Rho, Nucl. Phys. A **596**, 515 (1996), arXiv:nucl-th/9505017.

[10] S. Kölling, E. Epelbaum, H. Krebs, and U.-G. Meißner, Phys. Rev. C **80**, 045502 (2009), arXiv:0907.3437 [nucl-th].

[11] S. Kölling, E. Epelbaum, H. Krebs, and U.-G. Meißner, Phys. Rev. C **84**, 054008 (2011), arXiv:1107.0602 [nucl-th].

[12] S. Pastore, L. Girlanda, R. Schiavilla, and M. Viviani, Phys. Rev. C **84**, 024001 (2011), arXiv:1106.4539 [nucl-th].

[13] A. Baroni, L. Girlanda, S. Pastore, R. Schiavilla, and M. Viviani, Phys. Rev. C **93**, 015501 (2016), [Erratum: Phys. Rev. C **93**, 049902 (2016), Erratum: Phys. Rev. C **95**, 059901 (2017)], arXiv:1509.07039 [nucl-th].

[14] H. Krebs, Eur. Phys. J. A **56**, 234 (2020), arXiv:2008.00974 [nucl-th].

[15] M. Hoferichter, P. Klos, and A. Schwenk, Phys. Lett. B **746**, 410 (2015).

[16] V. Cirigliano, W. Dekens, J. de Vries, M. L. Graesser, and E. Mereghetti, JHEP **2018**, 97 (2018).

[17] F. Oosterhof, B. Long, J. de Vries, R. G. E. Timmermans, and U. van Kolck, Phys. Rev. Lett. **122**, 172501 (2019), arXiv:1902.05342 [hep-ph].

[18] T.-X. Liu, R. Peng, S. Lyu, and B. Long, Phys. Rev. C **106**, 055501 (2022), arXiv:2207.04241 [nucl-th].

[19] A. Nogga, R. G. E. Timmermans, and U. van Kolck, Phys. Rev. C **72**, 054006 (2005), arXiv:nucl-th/0506005.

[20] M. Pavon Valderrama, Phys. Rev. C **84**, 064002 (2011), arXiv:1108.0872 [nucl-th].

[21] B. Long and C. J. Yang, Phys. Rev. C **84**, 057001 (2011), arXiv:1108.0985 [nucl-th].

[22] W. Shi, R. Peng, T.-X. Liu, S. Lyu, and B. Long, Phys. Rev. C **106**, 015505 (2022).

[23] B. Long and C. J. Yang, Phys. Rev. C **85**, 034002 (2012),

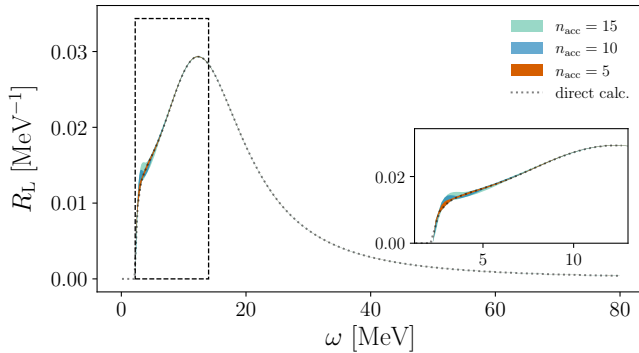


Figure 8. Deuteron response from the inverted LIT $\Lambda = 800$ MeV, $\sigma_I = 3.0$ MeV for momentum transfer $q^2 = 1.0$ fm $^{-2}$.

arXiv:1111.3993 [nucl-th].

[24] B. Long and C. J. Yang, Phys. Rev. C **86**, 024001 (2012), arXiv:1202.4053 [nucl-th].

[25] S. Wu and B. Long, Phys. Rev. C **99**, 024003 (2019), arXiv:1807.04407 [nucl-th].

[26] M. Pavón Valderrama and D. R. Phillips, Phys. Rev. Lett. **114**, 082502 (2015), arXiv:1407.0437 [nucl-th].

[27] V. D. Efros, W. Leidemann, and G. Orlandini, Phys. Lett. B **338**, 130 (1994).

[28] V. D. Efros, W. Leidemann, G. Orlandini, and N. Barnea, J. Phys. G: Nucl. Part. Phys. **34**, R459 (2007), publisher: IOP Publishing.

[29] F. Marino, F. Bonaiti, S. Bacca, G. Hagen, and G. R. Jansen, (2025), arXiv:2504.11012 [nucl-th].

[30] H. W. Griesshammer, J. Liao, J. A. McGovern, A. Nogga, and D. R. Phillips, Eur. Phys. J. A **60**, 132 (2024), arXiv:2401.16995 [nucl-th].

[31] T. de Forest Jr. and J. Walecka, Advances in Physics **15**, 1 (1966).

[32] J. Carlson and R. Schiavilla, Rev. Mod. Phys. **70**, 743 (1998), publisher: American Physical Society.

[33] S. Bacca and S. Pastore, Journal of Physics G: Nuclear and Particle Physics **41**, 123002 (2014).

[34] S. Martinelli, H. Kamada, G. Orlandini, and W. Glöckle, Phys. Rev. C **52**, 1778 (1995), publisher: American Physical Society.

[35] S. Bacca, *Study of electromagnetic reactions on light nuclei with the Lorentz Integral Transform method*, Ph.D. Thesis, Johannes Gutenberg-Universität Mainz, Mainz (2005).

[36] V. D. Efros, W. Leidemann, and G. Orlandini, Few-Body Syst. **14**, 151 (1993).

[37] E. Epelbaum, W. Glöckle, and U.-G. Meißner, Nucl. Phys. A **671**, 295 (2000), arXiv:nucl-th/9910064.

[38] X. Kong and F. Ravndal, Nucl. Phys. A **665**, 137 (2000), arXiv:hep-ph/9903523.

[39] D. B. Kaplan, Phys. Rev. C **102**, 034004 (2020), arXiv:1905.07485 [nucl-th].

[40] W. Frank, D. J. Land, and R. M. Spector, Rev. Mod. Phys. **43**, 36 (1971).

[41] “The nn-online,” <http://nn-online.org>.

[42] V. G. J. Stoks, R. A. M. Klomp, M. C. M. Rentmeester, and J. J. de Swart, Phys. Rev. C **48**, 792 (1993).

[43] M. Pavón Valderrama, M. Sánchez Sánchez, C. J. Yang, B. Long, J. Carbonell, and U. van Kolck, Phys. Rev. C **95**, 054001 (2017), arXiv:1611.10175 [nucl-th].

[44] D. R. Phillips, Phys. Lett. B **567**, 12 (2003).

[45] H. Krebs, E. Epelbaum, and U.-G. Meißner, Few-Body Syst. **60**, 31 (2019).

[46] R. Schiavilla and V. R. Pandharipande, Phys. Rev. C **65**, 064009 (2002), arXiv:nucl-th/0201043.

[47] S. N. More, S. König, R. J. Furnstahl, and K. Hebeler, Phys. Rev. C **92**, 064002 (2015), arXiv:1510.04955 [nucl-th].

[48] S. N. More, S. K. Bogner, and R. J. Furnstahl, Phys. Rev. C **96**, 054004 (2017), arXiv:1708.03315 [nucl-th].

[49] G. G. Simon, F. Borkowski, Ch. Schmitt, V. H. Walther, H. Arenhövel, and W. Fabian, Nucl. Phys. A **324**, 277 (1979).

[50] W. Fabian and H. Arenhövel, Nucl. Phys. A **314**, 253 (1979).

[51] H. Arenhövel, W. Leidemann, and E. L. Tomusiak, Eur. Phys. J. A **23**, 147 (2005).

[52] S. Christlmeier and H. W. Griesshammer, Phys. Rev. C **77**, 064001 (2008), arXiv:0803.1307 [nucl-th].

[53] Y. P. Teng and H. W. Griesshammer, Eur. Phys. J. A **61**, 211 (2025), arXiv:2410.09653 [nucl-th].

[54] S. Lyu, L. Zuo, R. Peng, S. König, and B. Long, (2025), arXiv:2511.12522 [nucl-th].

[55] S. König, Eur. Phys. J. A **56**, 113 (2020).

[56] R. Peng, S. Lyu, S. König, and B. Long, Phys. Rev. C **105**, 054002 (2022), arXiv:2112.00947 [nucl-th].

[57] S. Bacca, N. Barnea, W. Leidemann, and G. Orlandini, Phys. Rev. Lett. **110**, 042503 (2013), publisher: American Physical Society.

[58] S. Kegel *et al.*, Phys. Rev. Lett. **130**, 152502 (2023), arXiv:2112.10582 [nucl-ex].

[59] N. Michel, W. Nazarewicz, and M. Płoszajczak, Phys. Rev. Lett. **131**, 242502 (2023), [Erratum: Phys. Rev. Lett. 133, 239901 (2024)], arXiv:2306.05192 [nucl-th].

[60] U.-G. Meißner, S. Shen, S. Elhatisari, and D. Lee, Phys. Rev. Lett. **132**, 062501 (2024), arXiv:2309.01558 [nucl-th].

[61] P. Yin, A. M. Shirokov, H. Li, B. Zhou, X. Zhao, S. Bacca, and J. P. Vary, Phys. Rev. C **112**, L031303 (2025), arXiv:2412.18037 [nucl-th].

[62] W. Glöckle, *The Quantum Mechanical Few-Body Problem* (Springer, Berlin; New York, 1983).

[63] D. A. Varshalovich, A. N. Moskalev, and V. K. Khersonskii, *Quantum Theory of Angular Momentum: Irreducible Tensors, Spherical Harmonics, Vector Coupling Coefficients, 3nj Symbols* (World Scientific Publishing Company, 1988).

[64] M. Hjorth-Jensen, “Applied data analysis and machine learning,” <https://compphysics.github.io/MachineLearning/doc/LectureNotes/> (2023).